ATTENUATION OF HIPPOCAMPAL TOXICITY IN MANGANESE CHLORIDE-EXPOSED WISTAR RATS TREATED WITH VANILLIN

BY

EKHOSUEHI NATASHA IYOBOSA
BMS2101321

SUPERVISOR:

DR. A. B. ENOGIERU

DEPARTMENT OF ANATOMY
SCHOOL OF BASIC MEDICAL SCIENCES
COLLEGE OF MEDICAL SCIENCES

UNIVERSITY OF BENIN

NOVEMBER, 2025.

ATTENUATION OF HIPPOCAMPAL TOXICITY IN MANGANESE CHLORIDE-EXPOSED WISTAR RATS TREATED WITH VANILLIN

BY

EKHOSUEHI NATASHA IYOBOSA
BMS2101321

A PROJECT SUBMITTED TO THE DEPARTMENT OF ANATOMY, SCHOOL OF BASIC MEDICAL SCIENCES, COLLEGE OF MEDICAL SCIENCES, UNIVERSITY OF BENIN, BENIN CITY.

IN PARTIAL FULFILLMENT FOR THE AWARD OF BACHELOR OF SCIENCE (BSc.) DEGREE IN ANATOMY OF THE UNIVERSITY OF BENIN, BENIN CITY

NOVEMBER, 2025

DECLARATION

I declare that:

1. This project report is based on the experimental work undertaken by me in the Department of Anatomy, University of Benin, under the supervision of Dr. Adaze B. Enogieru.
2. This work has not been previously submitted for the award of a degree elsewhere.
3. All ideas and views are essentially based on this research. And where the views of others have been expressed, such words were duly acknowledged.

____

EKHOSUEHI NATASHA IYOBOSA

BMS2101321

CERTIFICATION

This is to certify that this project work titled "**ATTENUATION OF HIPPOCAMPAL TOXICITY IN MANGANESE CHLORIDE-EXPOSED WISTAR RATS TREATED WITH VANILLIN**" was carried out by **EKHOSUEHI NATASHA IYOBOSA** in the Department of Anatomy, School of Basic Medical Sciences, University of Benin, Benin City, Nigeria.

____________________________ ________________

ADAZE B. ENOGIERU (PhD) **DATE**

Supervisor

____________________________ ________________

ADAZE B. ENOGIERU (PhD) **DATE**

Head of Department

____________________________ ________________

EXTERNAL EXAMINER **DATE**

DEDICATION

This work is dedicated to God the Father, God the Son and God the Holy Spirit.

ACKNOWLEDGEMENT

First and foremost, I give all glory, honor, and praise to God Almighty for His grace, wisdom, strength, and guidance throughout the course of this research and my academic journey. Without Him, this work would not have been possible.

I express my heartfelt appreciation to my supervisor, Dr. A. B. Enogieru, for his invaluable guidance, encouragement, and patience. His expert advice, constructive criticism, and continuous support were instrumental to the success of this research. My deepest gratitude goes to my beloved parents, Engr. and Mrs. Charles Uwadiae Ekhosuehi, for their unwavering love, prayers, and sacrifices that have brought me thus far. Your constant motivation and belief in me have been my greatest source of strength. I would also love to give a shout out to my siblings, Pharez and Charisse Ekhosuehi, for their motivation and love during the course of this research.

Special thanks to my colleagues and research partners, Chelsea and Monalisa—fondly known as “The Vanillin Girls”—for their teamwork, dedication, and friendship throughout this project. Working with you both made the experience truly enjoyable and memorable. I also extend my warm appreciation to my darling Aunty Patricia and her husband, Mattieu Distel, for their kindness, encouragement, and support during the course of this study. Finally, I acknowledge the Department of Anatomy, University of Benin, for providing the facilities and enabling environment that made this research possible.

TABLE OF CONTENTS

ABSTRACT

Hippocampal dysfunction, often linked to learning and memory impairments, can result from neurodegeneration or exposure to toxic agents. Manganese chloride, a neurotoxic compound, accumulates in the hippocampus and disrupts neuronal signalling through oxidative stress, mitochondrial dysfunction, and inflammation, leading to cognitive deficits. Vanillin, a natural phenolic compound with antioxidant and anti-inflammatory properties, has shown potential in protecting against such neurotoxic damage and preserving hippocampal integrity. Accordingly, the aim of this study was to evaluate the activity of vanillin on manganese chloride-induced hippocampal toxicity in Wistar rats. Forty-eight (48) adult Wistar rats were randomly assigned into six groups (A-F). Group A served as control; Group B received 10 mg/kg body weight [BW] of manganese chloride only; Group C received 20 mg/kg BW of vanillin and 10 mg/kg BW of manganese chloride. Group D received 40 mg/kg BW of vanillin and 10 mg/kg BW of manganese chloride. Group E received 20 mg/kg BW of vanillin only and Group F received 40 mg/kg BW of vanillin only. All administrations, lasted for twenty-eight (28) days. Nneurobehavioral activities were evaluated using the Novel object recognition and elevated plus maze tests. Following the sacrifice of the experimental rats, the hippocampi were collected for antioxidant enzymes activity, lipid peroxidation, and histological assessments. Results from this study showed that manganese chloride-exposed rats exhibited significant ($p < 0.05$) brain and body weight loss, cognitive and memory impairments, disrupted antioxidant enzyme activity, increased lipid peroxidation, along with atrophy and vacuolation of pyramidal cells and astrocytes in the CA1 region. Conversely, pre-treatment with vanillin mitigated weight loss, oxidative imbalance, lipid peroxidation, and neuronal damage. Overall, these findings suggest that Vanillin exhibits antioxidant properties against manganese chloride-induced neurotoxicity, thus making it a promising agent with potential against hippocampal dysfunction.

CHAPTER ONE

INTRODUCTION

1.1 BACKGROUND OF THE STUDY

Environmental exposure to heavy metals remains a global health concern, as these elements can accumulate in vital organs and disrupt normal physiological functions (Ohiagu *et al*., 2022; Jomova *et al*., 2025). Among them, manganese (Mn) occupies a unique position. Although it is an essential trace element required for enzymatic activity, antioxidant defense, and neuronal metabolism, excessive exposure has been strongly linked to neurotoxicity (Jomova *et al*., 2025). Occupational settings, contaminated food, and polluted water represent major sources of Mn overload, which has been associated with neurological syndromes resembling Parkinson's disease (Ohiagu *et al*., 2022).

The hippocampus, a critical brain region responsible for learning, memory, and spatial navigation, is particularly vulnerable to Mn-induced neurotoxicity (Peres *et al*., 2016; Dos Santos *et al*., 2017). Excessive accumulation of Mn in hippocampal neurons disrupts neurotransmitter balance, impairs synaptic plasticity, and interferes with neurogenesis (Dos Santos *et al*., 2017). Mn exposure promotes oxidative stress through the excessive generation of reactive oxygen species (ROS), mitochondrial dysfunction, and depletion of endogenous antioxidant defenses (Singh *et al*., 2019; Sachdev *et al*., 2021). These processes culminate in lipid peroxidation, protein oxidation, DNA damage, and ultimately neuronal apoptosis. In parallel, Mn-induced activation of inflammatory pathways elevates cytokines, which further aggravate hippocampal damage and cognitive decline (Peres *et al*., 2016; Sachdev *et al*., 2021).

Given the central role of oxidative stress and inflammation in Mn neurotoxicity, attention has shifted towards natural compounds with antioxidant and neuroprotective properties. Vanillin, the primary phenolic aldehyde in vanilla beans (*Vanilla planifolia*), has gained interest beyond its traditional use as a flavouring agent (Gallage and Møller, 2017; Arya *et al*., 2021). Experimental studies have demonstrated that vanillin exhibits strong free-radical scavenging activity, suppresses lipid peroxidation, and enhances endogenous antioxidant enzymes such as superoxide dismutase (SOD) and catalase (Gallage and Møller, 2017; Kim *et al*., 2019). Additionally, vanillin modulates inflammatory signalling pathways, reducing the expression of pro-inflammatory cytokines and protecting neurons from excitotoxic injury (Kim *et al*., 2019; Arya *et al*., 2021; Kafali *et al*., 2024).

1.2 STATEMENT OF RESEARCH PROBLEM

Manganese is an essential trace element required for normal physiological processes, including enzymatic activity, antioxidant defense, and neurotransmitter synthesis (Jomova *et al*., 2025). However, chronic exposure to elevated levels of Mn has emerged as a major public health concern due to its neurotoxic potential (Peres *et al*., 2016). Sources of Mn overload include contaminated water, polluted air, industrial emissions, and occupational settings such as mining and welding (Dey *et al*., 2023). Unlike many other metals, Mn readily accumulates in the brain, where excessive concentrations disrupt neuronal function and increase the risk of neurodegenerative outcomes (Dey *et al*., 2023; Jomova *et al*., 2025).

The hippocampus, a key structure responsible for learning, memory, and cognitive processing, is particularly susceptible to Mn-induced neurotoxicity (Peres *et al*., 2016). Evidence indicates that Mn overload impairs synaptic plasticity, disrupts neurotransmitter regulation, and interferes with hippocampal neurogenesis, ultimately leading to memory deficits and cognitive decline (Dey *et al*., 2023; Cheng *et al*., 2023). These detrimental effects are strongly associated with oxidative stress and inflammation, as Mn exposure enhances the generation of reactive oxygen species (ROS), disrupts mitochondrial function, and activates proinflammatory cytokines (Cheng *et al*., 2023; Jomova *et al*., 2025). Neuronal apoptosis, lipid peroxidation, and DNA damage further contribute to hippocampal degeneration.

Despite growing recognition of the neurological hazards of Mn exposure, current therapeutic approaches are limited and largely symptomatic. Chelation therapy offers only partial benefits and is often associated with adverse side effects (Aaseth and Nurchi, 2022). There is therefore a pressing need to identify safe, affordable, and effective neuroprotective strategies capable of targeting both oxidative and inflammatory pathways involved in Mn-induced hippocampal damage.

1.3 AIM OF THE STUDY

The aim of this study was to investigate the activity of vanillin on Manganese chloride-induced cerebral toxicity in adult Wistar rats.

1.4 SPECIFIC OBJECTIVES

The specific objectives of the study are to investigate the activity of vanillin on:

i. the brain and body weight changes in rats treated with or without manganese chloride
ii. the neuro-behavioural activity (novel object recognition and elevated plus maze tests) of rats treated with or without manganese chloride
iii. the antioxidant enzymes (superoxide dismutase, catalase, glutathione peroxidase) activity in the hippocampus of rats treated with or without manganese chloride.
iv. the lipid peroxidation (malondialdehyde concentration) in the hippocampus of rats treated with or without manganese chloride.
v. the histology of the hippocampus of rats treated with or without manganese chloride.

1.5 JUSTIFICATION OF THE STUDY

Phytotherapy, particularly the use of natural compounds with established pharmacological activities, has emerged as a promising strategy in combating heavy metal–induced toxicity (Flora *et al*., 2013; Rajak *et al*., 2020). Among these, vanillin, the major bioactive compound of *Vanilla planifolia*, stands out as a potential candidate. Traditionally valued as a flavouring agent, vanillin has gained increasing recognition for its pharmacological benefits, including antioxidant, anti-inflammatory, anti-apoptotic, and neuroprotective activities (Gallage and Møller, 2017; Arya *et al*., 2020). Importantly, oxidative stress and chronic inflammation are central mechanisms in Mn-induced hippocampal injury (Harischandra *et al*., 2019; Wang *et al*., 2020). The hippocampus, due to its high metabolic demand and dense neuronal connectivity, is particularly vulnerable to reactive oxygen species (ROS), leading to lipid peroxidation, DNA damage, and neuronal apoptosis (Harischandra *et al*., 2019). Vanillin, with its ability to scavenge free radicals, enhance endogenous antioxidant defenses, and suppress pro-inflammatory cytokines (Arya *et al*., 2020) offers a promising neuroprotective pathway against Mn toxicity.

Despite these promising properties, there remains a paucity of scientific data specifically addressing the protective role of vanillin in Mn-induced hippocampal dysfunction. Thus, this study is justified not only by its scientific contribution in filling this knowledge gap but also by its potential socioeconomic and public health relevance. In resource-limited settings, where heavy metal exposure remains poorly regulated due to industrial activities, mining, and waste mismanagement, validating affordable, plant-based interventions could provide culturally acceptable, accessible, and sustainable neuroprotective options. Furthermore, this study promotes the evidence-based use of natural compounds, contributing to both global health equity and the development of integrative neurotherapeutics.

CHAPTER TWO

LITERATURE REVIEW

2.1 THE BRAIN

The brain is a vital and highly intricate organ that forms the central component of the central nervous system. It is well protected within the bony structure of the skull, known as the neurocranium (Bhushan *et al*., 2022). Anatomically, the brain is divided into three major regions, each with distinct functions. The cerebrum is responsible for higher cognitive processes such as thought, memory, and reasoning. The cerebellum plays a central role in coordinating motor activity and maintaining balance, while the brainstem regulates automatic, life-sustaining functions such as breathing and cardiovascular control (Bhushan *et al*., 2022).

From an embryological standpoint, these divisions arise from the differentiation of three primary brain vesicles during early neural development. The forebrain, or prosencephalon, gives rise to the telencephalon, which develops into the paired cerebral hemispheres and neocortex, and the diencephalon, which forms the thalamus, hypothalamus, and metathalamus (Carstens and Sarnat, 2023). The midbrain, or mesencephalon, develops into the tectum, tegmentum, and cerebral peduncles (Carstens and Sarnat, 2023; Chakravarthi *et al*., 2025). Finally, the hindbrain, or rhombencephalon, differentiates into the metencephalon, which becomes the pons and cerebellum, and the myelencephalon, which gives rise to the medulla oblongata. Together, these structures form the foundation of the brain's functional architecture, supporting processes that range from higher cognition and sensory integration to motor coordination and the regulation of essential autonomic functions (Bhushan *et al*., 2022; Carstens and Sarnat, 2023).

2.2 THE HIPPOCAMPUS

2.2.1 Gross Anatomy of the Hippocampus

The hippocampus is a bilaterally curved structure of the cerebral cortex, located deep within the medial temporal lobe of each hemisphere (Chauhan *et al*., 2021). Also known as *cornu Ammonis* or Ammon's horn, it is an evolutionarily conserved allocortical region. During fetal development, the hippocampus undergoes a characteristic medial infolding, becoming embedded in the floor of the inferior (temporal) horn of the lateral ventricle. This process gives rise to its distinctive curved, C-shaped morphology, clearly visible in coronal sections (Catani, 2022; Lang *et al*., 2024). In the adult brain, the hippocampus appears as a longitudinal ridge along the temporal horn, maintaining continuity with the subiculum and parahippocampal gyrus, which connect it to the neocortex. Through these links, it plays a central role in memory consolidation and spatial navigation (Chauhan *et al*., 2021; Estela-Pro and Burwell, 2022).

Historically, the term "hippocampus" derives from the Greek words *hippos* (horse) and *kampos* (sea monster), reflecting its resemblance to a seahorse in coronal sections. This name was first introduced by Giulio Cesare Arantius (1530–1589), who noted its similarity to the marine creature (Estela-Pro and Burwell, 2022). Its alternative designation, *cornu Ammonis*, or "horn of Ammon," was inspired by the spiral horns of the Egyptian god Amun, further emphasizing its curved, ram's-horn shape (Bhushan *et al*., 2022; Chakravarthi *et al*., 2025).

Structurally, the anterior portion of the hippocampus is enlarged and marked by ridges referred to as the *pes hippocampi* ("foot of the hippocampus"), while posteriorly it tapers beneath the splenium of the corpus callosum, joining the crus of the fornix (Zhao and Palomero-Gallagher, 2025). Its principal output pathway begins with the alveus, a thin layer of white matter formed by axons of pyramidal neurons. These fibers converge into the fimbria, which continues as the fornix—the major efferent tract relaying hippocampal signals to thalamic, septal, and cortical regions (Estela-Pro and Burwell, 2022; Lang *et al*., 2024).

2.2.2 Organization of Pyramidal Cells in the Hippocampus

The cornu ammonis of the hippocampus is subdivided into four zones—CA1, CA2, CA3, and CA4—clearly visible in coronal sections (Kominami *et al*., 2023). CA1, also called Sommer's sector, lies adjacent to the subiculum, while CA2 and CA3 are positioned closer to the ventricular surface. A distinctive feature of CA3 is the Schaffer collaterals, recurrent axonal projections that form strong excitatory connections with CA1 neurons. CA4, situated within the hilus of the dentate gyrus, is often considered part of the dentate complex itself (Chauhan *et al*., 2021; Sheintuch *et al*., 2023).

The hippocampus is composed of archicortex, with pyramidal neurons forming its principal cell type. These neurons are characterized by extensive apical and basal dendrites that integrate excitatory and inhibitory inputs, and a single axon that contributes to hippocampal output (Sheintuch *et al*., 2023; Zhao and Palomero-Gallagher, 2025). Their axons form the alveus, converge into the fimbria, and then continue as the fornix. Through this alveus–fimbria–fornix pathway, hippocampal signals are widely distributed to the entorhinal and prefrontal cortices, septal nuclei, mammillary bodies, and anterior thalamic nuclei, supporting memory consolidation, spatial navigation, and limbic regulation (Cohen and Meyer, 2020; González-Arnay *et al*., 2024).

Structurally, the hippocampal archicortex is organized into four layers. The stratum lacunosum-moleculare, adjacent to the hippocampal fissure, contains inhibitory interneurons that regulate inputs from the entorhinal cortex. Beneath it, the stratum radiatum hosts apical dendrites of CA1 and CA3 neurons and receives Schaffer collateral inputs, forming a critical link in the trisynaptic circuit. At the core, the stratum pyramidale contains the densely packed pyramidal cell bodies that act as the main excitatory output. Finally, the stratum oriens, lying just below the alveus, contains basal dendrites of pyramidal cells as well as basket and oriens-lacunosum molecular (OLM) interneurons that fine-tune hippocampal activity (Genon *et al*., 2021; Estela-Pro and Burwell, 2022).

2.2.3 Hippocampal Connections

Sensory information reaches the hippocampus mainly through the perforant pathways, which arise from layer II of the lateral and medial entorhinal cortex. The lateral pathway projects to the outer molecular layer of the dentate gyrus, while the medial pathway targets the middle layer and also sends collaterals to CA3 and CA1 (Ohara *et al*., 2023; Vandrey *et al*., 2022). These inputs are rhythmically paced by a septohippocampal loop, where cholinergic and GABAergic projections from the medial septum regulate theta oscillations (Rolls and Treves, 2024). Additional modulatory signals come from prefrontal and cingulate cortices via the nucleus reuniens, and from the supramammillary nucleus, which together enhance synchrony and activity in CA2 and the dentate gyrus (Danieli *et al*., 2023). Ascending monoaminergic systems—including the locus coeruleus, raphe nuclei, and ventral tegmental area—provide widespread innervation that adjusts arousal, mood, and reward-linked memory consolidation (Rolls *et al*., 2022).

Hippocampal outputs arise primarily from CA1 and the subiculum, which project through the alveus, fimbria, and fornix. The precommissural fornix connects to the lateral septum, while the postcommissural branch innervates the mammillary bodies and anterior thalamic nuclei, completing the Papez circuit (Kamali *et al*., 2023). In parallel, amygdalar projections travel via the stria terminalis and ventral amygdalofugal pathway to hypothalamic and brainstem targets. Subicular collaterals return signals to entorhinal, cingulate, and prefrontal cortices, while the hippocampal commissure interlinks the two hemispheres (Ohara *et al*., 2023). Together, these afferent and efferent networks ensure the hippocampus integrates sensory, mnemonic, and emotional information across limbic, diencephalic, and cortical systems (Turner *et al*., 2022; Rolls and Treves, 2024).

2.2.4 Blood Supply and Drainage of the Hippocampus

The hippocampus receives its arterial supply primarily from branches of the posterior cerebral artery (PCA) and the anterior choroidal artery (AChA) (Xu *et al*., 2021). The PCA, especially its P2 segment, gives rise to anterior and posterior hippocampal arteries and contributes via posterior parahippocampal and parieto-occipital branches, supplying the entorhinal cortex and parahippocampal gyrus—key regions for memory processing (Agarwal and Carare, 2021; Xu *et al*., 2021). The AChA, a branch of the internal carotid artery, supplies the hippocampal head, uncus, and amygdala, as well as the choroid plexus, optic tract, and posterior limb of the internal capsule, highlighting its role in memory and sensorimotor function (Lucifero *et al*., 2021; Mithani *et al*., 2020). Within the hippocampus, arteries branch into ventral and dorsal groups, each targeting specific layers: for instance, large ventral branches supply the stratum lacunosum, stratum pyramidale, and dentate molecular layer, while dorsal branches perfuse the granule cell layer and CA3/CA4 subfields. These vessels form a longitudinally anastomotic network along the hippocampal sulcus, enhancing resilience to ischemia (Thorne *et al*., 2022; Semyachkina-Glushkovskaya *et al*., 2023).

Venous drainage occurs via superficial and deep systems. Deep veins, including sulcal intrahippocampal and subependymal veins, drain CA1–CA4 and subiculum, connecting to superficial arcades along the fimbriodentate and hippocampal sulci. These arcades converge anteriorly into the inferior ventricular vein and posteriorly into the medial atrial vein, ultimately joining the basal vein of Rosenthal to clear venous blood from the medial temporal lobe (Inoue *et al*., 2023; Ota, 2024). This vascular architecture ensures metabolic homeostasis and protects against ischemic injury, with variations in arterial and venous patterns contributing to individual differences in hippocampal perfusion and susceptibility to neurodegeneration (Semyachkina-Glushkovskaya *et al*., 2023).

2.2.5 Functions of the Hippocampus

The hippocampus, a central component of the limbic system, plays a critical role in learning, memory, and spatial navigation (Chauhan *et al.*, 2021). In memory processing, its principal subfields (CA1–CA3) form a trisynaptic loop: perforant-path inputs from the entorhinal cortex excite dentate granule cells, which activate CA3 pyramidal neurons; CA3 then projects via Schaffer collaterals to CA1, before outputs return to neocortical regions. A direct temporoammonic pathway from layer III of the entorhinal cortex to CA1 supports rapid encoding of episodic events. Synaptic plasticity in these circuits, especially NMDA receptor–dependent long-term potentiation (LTP), underpins learning, memory consolidation, and pattern completion (Slotnick, 2022; Vandrey *et al*., 2022; Donato *et al*., 2021).

In learning, the hippocampus encodes temporal and associative information, as seen in paradigms like eyeblink conditioning. CA1 pyramidal neurons adjust firing patterns to anticipate stimulus timing and magnitude, while coordinated theta and sharp-wave ripple oscillations reinforce memory traces and support transfer to neocortical regions (Buss *et al*., 2021; Crossley *et al*., 2024).

For spatial navigation, the hippocampus constructs an internal cognitive map. Place cells fire selectively when an animal occupies a specific location, integrating spatial, contextual, and behavioral cues. Oscillatory coordination and synaptic plasticity ensure precise and stable spatial representations, which also provide a scaffold for episodic memory and future planning (Baumann and Mattingley, 2021; Etter *et al*., 2023).

Beyond cognition, the hippocampus guides goal-directed and adaptive behavior by forming relational memory representations that support flexible decision-making. It regulates inhibitory control, suppresses maladaptive responses, and integrates contextual and emotional information. Dysfunction or stress impairs hippocampal firing and plasticity, leading to deficits in learning, memory, and behavioral regulation (Uddin, 2021; Anderson and Floresco, 2022; Kalisch *et al*., 2024).

2.2.6 Hippocampal Disorders and Etiology

Hippocampal dysfunction is implicated in various neuropsychiatric and neurodegenerative disorders, including Alzheimer's disease (AD) and major depressive disorder (MDD). In AD, the hippocampus is among the first regions to degenerate, showing neuronal loss, gliosis, and atrophy across subfields such as CA1–CA4, the subiculum, and dentate layers (Salta *et al*., 2023; Rao *et al*., 2022). Pathologically, hyperphosphorylated tau accumulates into neurofibrillary tangles, spreading from the entorhinal cortex to the hippocampus and other cortical areas, while amyloid-beta plaques disrupt synaptic function and trigger neuronal death (Zhang *et al*., 2022). Dysregulation of glutamatergic, serotonergic, and noradrenergic systems further contributes to cognitive decline and behavioral disturbances (Okar *et al*., 2024). In depression, hippocampal volume is reduced, particularly in recurrent or early-onset cases, largely due to chronic glucocorticoid exposure and stress-induced downregulation of brain-derived neurotrophic factor (BDNF). These processes impair neurogenesis, dendritic architecture, and synaptic plasticity, leading to deficits in learning, memory, and emotional regulation (Tartt *et al*., 2022; Xiao *et al*., 2021). Glial dysfunction—including astrocyte loss, microglial activation, and oligodendrocyte deficits—further exacerbates hippocampal atrophy and cognitive symptoms (Shah *et al*., 2021).

Hippocampal disorders arise from diverse causes. Structural and genetic factors, such as congenital malformations, perinatal hypoxia, traumatic injury, strokes, or mutations in genes like SCN1A, MECP2, and DISC1, disrupt hippocampal architecture and circuitry, predisposing to epilepsy, cognitive deficits, or psychiatric symptoms (Wegrzyn *et al*., 2022). Autoimmune processes, as in limbic encephalitis, and infections, particularly HSV-1, selectively target hippocampal neurons, often leading to memory loss, seizures, or sclerosis (Wouk *et al*., 2021).

Toxic and metabolic insults—including chronic alcohol use, thiamine deficiency, hypoglycemia, electrolyte imbalance, or heavy metal exposure—can also induce hippocampal injury through excitotoxicity, oxidative stress, and synaptic loss (Eva *et al*., 2023; Liu *et al*., 2021).

2.3 MANGANESE

Manganese is an essential trace element, required in minute quantities to support normal cellular function, metabolism, and neurological health (Gurol *et al.*, 2022). It acts as a cofactor for several enzymes involved in carbohydrate, lipid, and protein metabolism and plays a pivotal role in antioxidant defense and neurotransmitter synthesis. It is the twelfth most abundant element in the earth's crust, typically found in ores such as pyrolusite and rhodochrosite (Balaram, 2022). Chemically, it exhibits multiple oxidation states, with Mn^{2+} and Mn^{3+} being the most biologically relevant. The ability to interchange between these states underlies its functional role in redox reactions and enzyme catalysis (Manavalan *et al.*, 2024). In the human body, manganese is normally present at concentrations tightly regulated by homeostatic mechanisms, with the adult brain containing approximately 0.25 µg/g wet weight (Gurol *et al.*, 2022).

Manganese was first identified as a distinct element in the late 18th century, and its industrial importance rapidly became apparent. By the 19th and 20th centuries, manganese had become indispensable in steel production, where it improved strength, durability, and resistance to wear (Balaram, 2022). During the same period, cases of manganese intoxication began to be documented among miners and industrial workers. While indispensable in small amounts, manganese can be toxic when present in excess. Chronic exposure, particularly via inhalation in occupational settings, can overwhelm the body's natural homeostatic controls (Obeng *et al.*, 2024).

2.3.1 Uses of Manganese

The industrial applications of manganese are diverse. It is a critical component in the manufacture of iron and steel alloys, where it enhances hardness and resistance to corrosion. It is also employed in the production of batteries, ceramics, glass, and pigments, as well as in fertilizers and fungicides (Balaram, 2022). In recent decades, organomanganese compounds such as methylcyclopentadienyl manganese tricarbonyl (MMT) have been used as fuel additives, although combustion by-products typically yield inorganic manganese oxides and salts (Obeng *et al.,* 2024). These wide-ranging uses result in widespread occupational and environmental exposure to manganese.

2.3.2 Routes of Exposure of Manganese

In the general population, manganese exposure is primarily dietary, with adults typically consuming between 0.7 and 10 mg per day through food and drinking water (Malik *et al.,* 2023). Vegetarians often have higher intakes due to manganese-rich plant sources such as grains, legumes, and nuts. Drinking water levels are usually low but can vary widely depending on geological conditions (Gomes and Silva, 2021).

In contrast, occupational exposure is dominated by inhalation of airborne dusts, fumes, or particulate matter, especially in mining, welding, and alloy production. Inhalation represents the most critical route in industrial environments because it can bypass gastrointestinal homeostatic controls (Fernández-Olmo *et al.,* 2020). Dermal exposure is considered negligible; as inorganic manganese compounds are poorly absorbed through the skin.

2.3.3 Absorption of Manganese

The efficiency of manganese absorption depends on both the route of entry and the chemical form. Soluble salts such as manganese chloride and sulphate are absorbed more readily than oxides or metallic forms (Yadav *et al.,* 2023). Oral absorption is relatively low, ranging between 3–13%, and is influenced by numerous factors: iron status, dietary composition, fasting, and the individual's existing body burden. Iron deficiency, for instance, enhances manganese uptake due to shared transport via transferrin (Baj *et al.,* 2023).

Inhalation provides a more efficient and concerning route of systemic exposure. In addition to pulmonary absorption, inhaled manganese particles may be transported directly to the brain via the olfactory nerve, bypassing the blood–brain barrier (Gurol *et al.,* 2022). This pathway has been demonstrated in rodents and primates, raising concerns about its relevance to human occupational exposure. Particle size and solubility strongly influence deposition and absorption within the respiratory tract (Gomes and Silva, 2021).

2.3.4 Distribution of Manganese

Once absorbed, manganese is distributed widely throughout the body. The liver acts as a key regulatory organ, clearing large fractions from portal blood following oral intake (Gandhi *et al.,* 2022). From the systemic circulation, manganese is transported primarily bound to transferrin, albumin, or alpha$_2$-macroglobulin. It readily crosses the placenta and accumulates in foetal tissues, highlighting the importance of maternal regulation (Baj *et al.,* 2023).

Particularly significant is manganese distribution to the brain. The element preferentially accumulates in basal ganglia regions such as the globus pallidus and striatum, areas critically involved in motor control (Pajarillo *et al.,* 2022). Inhalation exposure produces more pronounced brain deposition compared to oral intake, with measurable increases observed in primates without parallel rises in blood concentrations. This suggests additional routes of brain delivery beyond systemic circulation, consistent with olfactory transport mechanisms (Fernández-Olmo *et al.,* 2020).

2.3.5 Metabolism of Manganese

Manganese undergoes limited biochemical transformation but shifts between Mn^{2+} and Mn^{3+} states are crucial for binding and transport. Mn^{2+} is the primary absorbed form, which is subsequently oxidised to Mn^{3+} and bound to transferrin for systemic distribution (Manavalan *et al.,* 2024). Within tissues, manganese functions as a cofactor for numerous enzymes, including manganese superoxide dismutase (Mn-SOD), which plays a central role in mitochondrial oxidative defence. The oxidation state of manganese influences not only its toxicokinetics but also its toxicodynamics, with evidence suggesting that Mn^{3+} may exert more potent neurotoxic effects (Nyarko-Danquah *et al.,* 2020).

2.3.6 Excretion of Manganese

Elimination of manganese is governed largely by the hepatobiliary system. More than 95% of absorbed manganese is excreted via bile into the faeces, with urinary clearance accounting for less than 1% (Gurol *et al.,* 2022). Enterohepatic recirculation ensures that manganese elimination is tightly regulated, and increased intake stimulates enhanced excretion to maintain balance. Biological half-lives vary, with whole-body retention times of 30–40 days in humans. Clearance from the brain, however, is considerably slower due to the lack of active transport mechanisms out of the central nervous system (Pajarillo *et al.,* 2022).

2.3.7 Neurotoxic Effects of Manganese

Manganese is indispensable for normal brain development and function, yet excessive accumulation in neural tissues transforms it into a potent neurotoxin, particularly to neural circuits involved in motor control, cognition, and behaviour (Pajarillo *et al.,* 2022). Historically, emphasis was placed on its motor features, but recent advances have clarified that manganese neurotoxicity extends to complex cognitive and behavioural impairments. These outcomes arise from a combination of toxicokinetic properties (slow clearance, preferential brain accumulation) and toxicodynamic mechanisms (oxidative stress, neurotransmitter disruption, mitochondrial dysfunction, and neuroinflammation) (Tarnacka *et al.,* 2021).

Manganism classically presents with motor abnormalities such as dystonia, rigidity, tremor, and impaired gait. These manifestations stem largely from manganese deposition in the basal ganglia, particularly the globus pallidus, striatum, and substantia nigra (Kulshreshtha *et al.,* 2021). Unlike idiopathic Parkinson's disease, manganism does not primarily involve dopaminergic neuron loss, but rather altered neurotransmission and neuronal dysfunction within these nuclei. This explains the poor therapeutic response to L-DOPA in manganism patients (Tarnacka *et al.,* 2021). Instead of being rescued by dopamine replacement, motor circuits remain dysregulated due to manganese interference with presynaptic release, receptor sensitivity, and synaptic signaling (Chib and Singh, 2022).

Cognitive deficits are increasingly recognized as a hallmark of manganese neurotoxicity. Exposed individuals show impairments in executive functioning, including reduced working memory, slowed processing speed, and impaired problem-solving ability (Nyarko-Danquah *et al.,* 2020). Verbal fluency and sustained attention are also compromised, reflecting dysfunction in frontal–striatal circuits. Mechanistically, these impairments arise because manganese interferes with the dopaminergic and glutamatergic systems that underlie cognition. Manganese exposure reduces dopamine release in the prefrontal cortex and striatum, while simultaneously altering glutamate homeostasis, leading to excitotoxicity (Baj *et al.,* 2023). Disruption of these systems diminishes the efficiency of prefrontal cortical networks, impairing cognitive control. Functional imaging supports these findings, with manganese-exposed individuals showing abnormal activation patterns during tasks that require inhibitory control and working memory (Tarnacka *et al.,* 2021). Behavioural changes are often the most socially disruptive aspect of manganese toxicity. Irritability, mood instability, depression, apathy, and anxiety are frequently reported, while severe cases may include compulsivity, aggression, and psychotic features. The historical term *"manganese madness"* described miners who exhibited profound personality changes, aggression, and hallucinations after prolonged high-dose exposure (Richards and Richards, 2020).

Neurochemically, these behavioural effects stem from manganese-induced disturbances in dopamine and serotonin signaling within mesolimbic pathways. Excess manganese alters dopamine turnover in the nucleus accumbens and prefrontal cortex, impairing motivation and reward processing, while serotonergic dysregulation contributes to mood and anxiety disorders (Tarnacka *et al.,* 2021). Chronic exposure therefore destabilizes the neural substrates of emotional regulation and social behaviour.

2.3.8 Mechanistic Insights

2.3.8.1 Oxidative Stress and Redox Cycling

Manganese readily cycles between Mn^{2+} and Mn^{3+} states. While this property enables it to serve as a cofactor in antioxidant enzymes such as manganese superoxide dismutase (Mn-SOD), excess manganese promotes oxidative stress (Chandra and Roychoudhury, 2020). In its trivalent state (Mn^{3+}), manganese can generate reactive oxygen species (ROS) and disrupt mitochondrial respiration. Elevated ROS damages lipids, proteins, and DNA, particularly in vulnerable brain regions such as the basal ganglia and hippocampus, leading to neuronal dysfunction and death (Manavalan *et al.*, 2024).

2.3.8.2 Mitochondrial Dysfunction

Mitochondria are a primary target of manganese toxicity. Manganese accumulates within mitochondria due to its affinity for calcium transporters, where it impairs oxidative phosphorylation and ATP production (Fernandes *et al.,* 2023). This bioenergetic deficit compromises neuronal survival, especially in neurons with high metabolic demand such as dopaminergic cells. Moreover, mitochondrial manganese overload exacerbates ROS production and disrupts calcium homeostasis, triggering apoptotic pathways (Baj *et al.*, 2023).

2.3.8.3 Neurotransmitter Dysregulation

Manganese affects multiple neurotransmitter systems:

- ***Dopamine:*** Excess manganese disrupts dopamine synthesis, release, and receptor sensitivity in the basal ganglia and prefrontal cortex. This underlies both the motor deficits (via striatal dysfunction) and cognitive/behavioural impairments (via prefrontal hypodopaminergia) (Chib and Singh, 2022).
- ***Glutamate:*** Manganese inhibits astrocytic glutamate uptake, leading to extracellular glutamate accumulation and excitotoxicity. Overactivation of NMDA receptors further promotes oxidative and mitochondrial injury (Pajarillo *et al.,* 2022).
- ***GABA and Serotonin:*** Altered GABAergic and serotonergic transmission contributes to anxiety, depression, and irritability observed in exposed populations (Chib and Singh, 2022).

2.3.8.4 Neuroinflammation

Manganese activates microglia, the resident immune cells of the central nervous system, resulting in the release of pro-inflammatory cytokines (e.g., TNF-α, IL-6). Chronic microglial activation sustains a cycle of neuroinflammation, oxidative stress, and neuronal injury (Yan *et al.,* 2023). This is particularly detrimental in brain regions already burdened by manganese accumulation, amplifying neurodegeneration.

2.4 VANILLIN

Vanillin (4-hydroxy-3-methoxybenzaldehyde) is a well-known compound that typically appears as a white to slightly yellow crystalline powder. It is easily recognized by its pleasant, sweet fragrance, which has made it highly valuable in both food and fragrance industries (De and De, 2022). Physically, vanillin shows only moderate solubility in water at room temperature, although its solubility increases significantly in hot or boiling water. From a chemical standpoint, vanillin is classified as a phenolic aldehyde. Its structure contains three major functional groups: an aldehyde (R1), a hydroxyl (R2), and an ether (R3) (Raju *et al.,* 2023). The hydroxyl and ether groups together form the vanillyl (4-hydroxy-3-methoxybenzyl) backbone, a structural motif that is also found in several biologically active compounds collectively known as vanilloids. Examples of these include capsaicin, vanillylmandelic acid, gingerol, zingerone, vanillic acid, and eugenol (Raju *et al.,* 2023).

Naturally, vanillin is most abundant in species of the vanilla genus, particularly *Vanilla planifolia* Jacks. ex Andrews, *Vanilla tahitensis* J.W. Moore, and *Vanilla pompona* Schiede, all belonging to the Orchidaceae family (de Oliveira *et al.,* 2022). However, it is not restricted to vanilla plants alone. It has also been identified in a variety of other species such as rice (*Oryza sativa*, Poaceae), *Bruguiera gymnorhiza* (Rhizophoraceae), *Melia azedarach* (Meliaceae), oregano (*Origanum vulgare,* Lamiaceae), *Hemidesmus indicus* (Apocynaceae), and *Gastrodia elata* (Orchidaceae), among others. Historically, vanillin has been one of the key constituents of natural vanilla and has long been used worldwide as a flavouring agent in foods, beverages, and related products (Arya *et al.,* 2021).

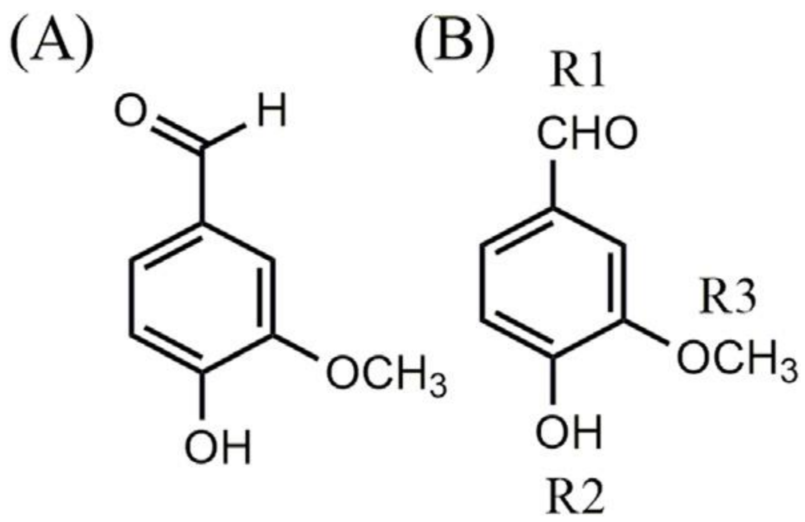

Figure 1: (A) Structure of vanillin (4-hydroxy-3-methoxybenzaldehyde), **(B)** Structure of vanillin showing the R moieties

2.4.1 Biosynthesis and Microbial Production of Vanillin

Vanillin is naturally synthesized in vanilla pods where it is stored in the form of a non-toxic glucoside, serving as a protective mechanism for the plant. Although the complete biosynthetic pathway of vanillin has not been fully elucidated, some key metabolic steps have been outlined. Kundu (2017) suggested that vanillin formation may proceed through multiple routes, including the modification of coniferin via C3 side-chain changes, CoA-dependent β-oxidative and non-β-oxidative processes, the conversion of 4-hydroxybenzyl alcohol glucoside to glucovanillin, a non-CoA-dependent non-β-oxidative pathway, as well as the direct enzymatic transformation of ferulic acid into vanillin.

Despite the availability of these biosynthetic precursors, traditional extraction of vanillin from vanilla plants cannot meet the global demand. This shortfall is largely due to low and unpredictable yields, the influence of climate variability, and labor-intensive processing methods (Tazon *et al.*, 2024). In fact, plant-derived vanillin accounts for only about 0.2% of the global supply, making large-scale reliance on natural sources impractical. Consequently, attention has shifted towards chemical and microbial production, with microbial synthesis often being favored due to its lower cost and environmentally friendly nature (Hayes *et al.*, 2022).

A wide range of microorganisms have been employed in microbial vanillin production, including *Pseudomonas* sp., *Amycolatopsis* sp., *Sphingomonas paucimobilis*, *Rhodococcus*, *Pseudomonas putida* KT2440, *Pseudomonas fluorescens*, *Streptomyces setonii*, and *Escherichia coli* (Ma *et al.*, 2022). These organisms share a central metabolic step: the conversion of ferulic acid to vanillin, catalyzed by two key enzymes—feruloyl-CoA synthetase (FCS) and enoyl-CoA hydratase/aldolase (ECH). In this pathway, ferulic acid is first activated to feruloyl-CoA by FCS, after which ECH catalyzes the hydration and cleavage of the intermediate to generate acetyl-CoA and vanillin (Fujimaki *et al.*, 2022).

Recent advances in metabolic engineering have introduced even more cost-effective microbial systems. For instance, genetically modified *E. coli* has been developed to use simple carbon sources such as glucose, glycerol, and xylose. Through the shikimate pathway, these sugars are converted into vanillic acid, which is subsequently reduced to vanillin via aryl aldehyde dehydrogenase (Tazon *et al.*, 2024). Similarly, yeasts such as *Saccharomyces cerevisiae* and *Schizosaccharomyces pombe* have been engineered to follow comparable pathways, with the addition of an aromatic carboxylic acid reductase gene to enhance intracellular processing and improve yields (Santos *et al.*, 2024).

With these advances in microbial biotechnology, vanillin can now be produced at significantly lower costs. This affordability, coupled with the versatility of its chemical scaffold, has stimulated growing interest in its potential pharmacological applications. As a result, vanillin has been increasingly studied not only as a flavoring compound but also as a bioactive molecule with therapeutic value across a wide spectrum of diseases and experimental models (Kafali *et al.,* 2024).

2.4.2 Applications of Vanillin

2.4.2.1 Foods and Beverages

Vanillin is extensively used as a flavour enhancer and sweetener in products such as chocolates, desserts, cakes, cookies, ice creams, soft drinks, baked goods, and liquors. The quantity added varies with the product type and desired flavour intensity; for instance, chocolate production typically uses about 20 g/100 kg, while biscuits and cookies may require around 35 g/100 kg (Arya *et al.,* 2021). In oven-baked goods, vanillin is often added after baking to prevent flavour loss at high temperatures. A common derivative is *vanillin sugar*, produced by blending sucrose with vanillin solution, widely used in baked products, ice creams, and doughs. In beverages, vanillin imparts a pleasant taste to soft drinks, wines, and chocolate-flavoured drinks. Beyond flavouring, its antimicrobial activity enhances food safety and shelf life (Kafali *et al.,* 2024).

2.4.2.2 Animal Feeds

In animal feeds, vanillin improves palatability by masking unpleasant odours and tastes from minerals, thereby encouraging intake and supporting growth. Its antimicrobial action further helps prevent undesirable smells caused by microbial contamination (Gaikwad *et al.,* 2024).

2.4.2.3 Perfumes and Cosmetics

Vanillin is a key fragrance chemical in perfumes and cosmetics, valued for masking odours and adding a smooth aroma. Its stability in formulations can be influenced by other raw materials such as cloves, orchids, or citrus derivatives, sometimes leading to discolouration. In soaps, high levels of vanillin may reduce foaming and cause colour changes. Ethyl vanillin is often preferred in such cases due to its reduced discolouration effect (Venkataraman *et al.,* 2024).

2.4.2.4 Pharmaceutical Products

Pharmaceutical applications of vanillin include its use as a flavouring excipient in syrups, suspensions, chewable tablets, and chewing gums, improving palatability and patient compliance (Kolling and Ghosh, 2021). At the low concentrations used, adverse interactions are rare. Vanillin has also served as a structural template in drug synthesis, contributing to the development of agents such as methyldopa (antihypertensive) and trimethoprim (antimicrobial for urinary tract infections) (Raju *et al.,* 2023).

2.4.2.5 Industrial Applications

Industrially, vanillin is employed as an antifoaming agent in lubricating oils, a UV stabilizer in plastics and rubbers, and in zinc coating and electroplating. It also functions as an attractant in insecticides, reduces mouth harshness in tobacco smoke, and acts as a catalyst in polymerization reactions (Arya *et al.,* 2021).

2.4.3 Bioavailability of Vanillin

The oral bioavailability of vanillin refers to the fraction of the compound that reaches systemic circulation in its active form. Despite its therapeutic potential, vanillin is limited by low bioavailability, short half-life, and extensive gastrointestinal metabolism, which restrict its application in medicine and health products (Raj and Singh, 2022). Studies reported that after oral administration (100 mg/kg bw), vanillin showed 7.6% bioavailability with a half-life of 10.3 h and peak plasma concentration at 4 h, whereas intravenous administration at the same dose was almost completely cleared within 2 h (Abdelmonem *et al.,* 2025). Strategies to improve absorption have been explored; for example, MX-1520 (provanillin) exhibited over 30-fold higher oral bioavailability than vanillin. Metabolic studies indicate that vanillin undergoes extensive conjugation and urinary excretion, mainly as vanillic acid (47%), vanillyl alcohol (19%), and vanilloyl glycine (19%) (Cox *et al.,* 2024). In the liver, it is oxidized to vanillic acid by aldehyde oxidase and further converted to protocatechuic acid via *O*-demethylation. Overall, oral administration appears to provide greater bioavailability than intraperitoneal routes, and differences in administration may account for variations reported in toxicity studies (Almostafa *et al.,* 2024).

2.4.4 Biological Properties of Vanillin

2.4.4.1 Anticancer Activity

Extensive research has demonstrated the potential of vanillin in preventing and treating cancer through diverse experimental models. Early studies showed that vanillin reduced mutations induced by methylmethane and mitomycin C in mouse bone marrow and *Drosophila melanogaster*, suggesting a protective role against genotoxicity (Razaq *et al.,* 2024). Similar antimutagenic effects were observed against mutagens such as N-ethyl-N-nitrosourea, N-methyl-N-nitrosourea, ethyl methanesulfonate, and bleomycin. In cancer cell studies, vanillin arrested the cell cycle at the G2/M and G0/G1 phases and triggered apoptosis in HT-29 colorectal cancer cells (IC50: 400 μg/ml), highlighting its relevance in colorectal cancer prevention (Kafali *et al.,* 2024). It also reduced UV-induced chromosomal abnormalities in Chinese hamster V79 lung cells, inhibited DNA-dependent protein kinase, and promoted DNA repair. Furthermore, it blocked the metabolic activation of carcinogens such as nitrosamines, HPB, NNAL, and NNK N-oxide in murine hepatic and pulmonary microsomes (Rakoczy *et al.,* 2021).

Vanillin has also been implicated in regulating tumor progression and metastasis. In human lung cancer cells, it suppressed metastasis by down-regulating Caveolin-1 (Cav-1), while in HepG2 liver cancer cells it inhibited MMP-9 activity through suppression of NF-κB signaling (Gu *et al.,* 2021). In hepatocarcinoma cells, it induced apoptosis and cell cycle arrest via decreased activity of activator protein-1 and ERK phosphorylation. Cytotoxic effects were also reported in A375 melanoma cells, where vanillin suppressed NF-κB activation, likely through its antioxidant and free radical scavenging properties (Kafali *et al.,* 2024; Pourhadi *et al.*, 2022).

Dietary inclusion of 1% vanillin in rats reduced tumor incidence and multiplicity in a multi-organ carcinogenesis model (Kapoor *et al.,* 2021). Importantly, vanillin acted synergistically with doxorubicin by modulating apoptosis-related markers (Bax/Bcl-2 ratio and caspase-9 activity) in MCF-7 breast cancer cells, suggesting value as both a standalone and adjuvant therapy (Rakoczy *et al.,* 2021). It also reduced mitomycin C-induced micronucleated erythrocytes by 50% in mice, reinforcing its cytotoxic and protective effects (Salimi *et al.,* 2024).

2.4.4.2 Antimicrobial Activity

Vanillin exhibits notable antimicrobial activity against a wide range of microorganisms, including bacteria, yeasts, and molds. In bacterial studies, concentrations between 10–40 mM were found to inhibit the growth of *E. coli*, *Lactobacillus plantarum*, and *Listeria innocua*, primarily through disruption of ion gradients and respiration, although *E. coli* showed reduced sensitivity with higher MIC values (Salam *et al.,* 2023; Arya *et al.,* 2021). Against fungi, its effects are more pronounced, with an average MIC of 5.71 mM reported for spoilage yeasts and molds. This antifungal property has been shown to effectively prevent microbial growth in soft drinks, fruit-based products, and bakery goods, thereby enhancing shelf life while maintaining taste and appearance (Li and Zhu, 2021).

Beyond its role in food preservation, vanillin has demonstrated medical potential. It inhibited pathogenic yeasts such as *Cryptococcus neoformans* and *Candida albicans*, with its activity attributed to the reactive aldehyde group (Raju *et al.*, 2023; Roy *et al.*, 2024). Vanillin isolated from *V. planifolia* pods also suppressed the growth of *Alternaria alternata*, a fungus of clinical and agricultural importance (Li and Zhu, 2021). Furthermore, chemical modifications of vanillin, particularly through the formation of Schiff bases, have resulted in derivatives with significantly improved antibacterial effects. These compounds have shown activity against both Gram-positive (*Staphylococcus aureus, Bacillus subtilis*) and Gram-negative (*Klebsiella pneumoniae*, *Pseudomonas aeruginosa*) bacteria, with some derivatives achieving MIC values as low as 125 µg/ml (Demirbağ *et al.*, 2025).

2.4.4.3 Antidepressant and Anxiolytic Activities

Depression is one of the most common mental health disorders, and studies using animal models have suggested that vanillin may play a useful role in its management (Iannuzzi *et al.,* 2023). In experimental models, behavioral tests such as the elevated plus maze, sucrose preference, and forced swim test (FST) have been applied to assess its activity. At a dose of 100 mg/kg body weight, vanillin significantly reduced immobility time in the FST and increased the time spent in the closed arm of the elevated plus maze in rats exposed to chronic mild stress (Du *et al.*, 2022). This was accompanied by biochemical changes, including elevated brain serotonin and reduced glutathione levels, together with decreased nitric oxide (NO) and malondialdehyde (MDA) levels (Wang *et al.*, 2024). Similarly, administration of vanillin at 10–100 mg/kg body weight decreased immobility in both the FST and the tail suspension test (TST) in a dose-dependent manner, with effects comparable to the standard antidepressant fluoxetine (Salau and Islam, 2024).

Beyond its antidepressant activity, vanillin also demonstrated anxiolytic effects. At doses ranging from 10–200 mg/kg body weight, it increased the number of rears in open arms, raised the percentage ratio of open-arm entries, and altered the time spent in closed arms, all of which are behavioral indicators of reduced anxiety (de Oliveira *et al.*, 2022; Kamaly *et al.*, 2025). Depression and anxiety are often linked with other neurological and physiological disorders, including sleep-related breathing problems such as apnea. Interestingly, vanillin was reported to reduce apnea episodes by more than threefold in premature newborns (Bergeron *et al.*, 2024).

2.4.4.4 Learning and Cognitive Potentials

Plant-derived bioactive compounds are increasingly recognized for their potential to enhance brain function, including learning, memory, and cognition. Vanillin has been studied in this context using animal models of cognitive impairment. In mice with scopolamine-induced amnesia, oral administration of vanillin at 40 mg/kg body weight for 28 days improved deficits in learning and memory (Gul *et al.*, 2024). These effects were associated with enhanced neuroblast differentiation and increased cell proliferation in the dentate gyrus of the hippocampus, suggesting that vanillin can stimulate endogenous neuronal regeneration and support cognitive processes (Iannuzzi *et al.*, 2023).

Further studies have indicated that vanillin may protect the brain against injury-induced dysfunction. Specifically, it improved the expression of inhibitor of DNA-binding protein 1 (ID1) in scopolamine-treated mice, mitigating the cognitive deficits associated with ID1 suppression (Anand *et al.,* 2022). This suggests that vanillin not only enhances neurogenesis but also helps maintain the functional integrity of neurons under stress or injury (Kafali *et al.,* 2024).

2.4.4.5 Neuroprotective Activity

Numerous studies have highlighted the neuroprotective potential of vanillin. In vitro, pretreatment of rotenone-induced SH-SY5Y neuroblastoma cells with vanillin demonstrated protection against apoptosis and mitochondrial dysfunction, primarily through activation of the c-Jun N-terminal kinase (JNK)-mitogen-activated protein kinase (MAPK) and p38 signaling pathways (Arya *et al.,* 2021; Iannuzzi *et al.,* 2023). These findings were confirmed in vivo, where administration of vanillin at 5–20 mg/kg body weight in a rotenone-induced Parkinson's disease rat model mitigated neurochemical deficits, reduced apoptosis, improved motor and non-motor impairments, and alleviated oxidative stress (Rani and Mondal, 2024).

Vanillin has also shown neuroprotective effects in models of nerve and spinal cord injury. Treatment with 150 mg/kg body weight for one week enhanced intramuscular vascularization in the tibialis anterior and soleus muscles of rats following nerve injury (Salau and Islam, 2024). Similarly, intraperitoneal administration at 286 mg/kg improved outcomes in rats with spinal cord injury, reducing motor dysfunction, oxidative stress, hypoxia-inducible factor-1α-positive cells, and TUNEL-positive apoptotic cells (Chen *et al.,* 2022).

Additional mechanisms of neuroprotection include inhibition of butyrylcholinesterase and acetylcholinesterase activities, as well as attenuation of oxidative damage in brain tissues exposed to Fe^{2+}-induced toxicity (Salau and Islam, 2024). A study also reported that vanillin at 50–100 mg/kg body weight reduced allodynia in rats, suggesting potential benefits for managing neuropathic pain, although hyperalgesia was unaffected (Kamaly *et al.,* 2025).

2.4.4.6 Hepatoprotective and Nephroprotective Activities

Vanillin has also demonstrated significant hepatoprotective and nephroprotective properties. In mice, the compound exhibited anti-hepatotoxic effects against potassium bromate-induced liver damage by reducing serum transaminases, lipid peroxidation, protein carbonyl content, and advanced oxidation protein products, while also improving the overall architecture of the liver (Alamri *et al.,* 2022; Afolabi *et al.,* 2023). Similarly, intraperitoneal administration of vanillin at 150 mg/kg body weight protected against carbon tetrachloride (CCl_4)-induced hepatotoxicity in rats. This effect was associated with decreased serum transaminase levels, enhanced protein content, inhibition of hepatic protein carbonyl formation and lipid peroxidation, improved liver structure, and strengthened antioxidant defenses (Alamri *et al.,* 2022).

In addition to liver protection, vanillin demonstrated nephroprotective activity. At 150 mg/kg body weight, it mitigated cisplatin- and methotrexate-induced kidney injury by reducing serum markers such as creatinine, cystatin C, and neutrophil gelatinase-associated lipocalin, as well as lowering kidney tissue levels of malondialdehyde, iNOS, TNF-α, IL-18, NF-κB p65, cytosolic cytochrome C, and caspase-3 (Afolabi *et al.*, 2023). Pretreatment also improved renal total antioxidant capacity and the Bcl-2/Bax ratio, while histopathological changes and Fas ligand expression in the kidneys were markedly ameliorated (Fouad and Al-Melhim, 2018). Even at a lower dose of 100 mg/kg, vanillin significantly protected against cisplatin-induced nephrotoxicity by reducing fibrotic markers such as TGF-β1 and fibroblast growth factor-23 (FGF-23), normalizing serum creatinine and urea, and preserving kidney integrity (Younis *et al.,* 2020).

2.4.4.7 Cardio-protective Activity

Vanillin has been extensively investigated for its cardioprotective potential. Initial studies demonstrated that the compound induced dose-dependent relaxation of coronary arteries contracted with endothelin-1, KCl, or U46619, a thromboxane A_2 receptor agonist (Yalameha *et al.,* 2023). Importantly, vanillin was able to abrogate contractions mediated by calcium influx and protein kinase C modulators, indicating a direct regulatory effect on vascular smooth muscle tone and suggesting its potential to alleviate vasospasms in coronary and cerebral arteries (Choi *et al.,* 2022).

Complementary studies provided in vivo evidence of cardioprotection, showing that oral administration of vanillin at 100 mg/kg body weight reduced cardiac protein oxidation and lipid peroxidation in mice, while improving cardiac morphology and structural integrity (Elseweidy *et al.,* 2023). These effects highlight the compound's ability to protect the heart from oxidative stress–induced damage and to preserve normal cardiac function.

2.4.4.8 Antioxidant, Anti-inflammatory and Analgesic Activities

Vanillin has been widely recognized for its antioxidant properties. In vitro studies have shown that it effectively scavenges a variety of free radicals, including DPPH (IC_{50}: 0.61 μM), hydroxyl radicals (IC_{50}: 0.16 μM), and superoxide anion radicals (IC_{50}: 2.95 mM and 2.33 μM), while also inhibiting lipid peroxidation with IC_{50} values ranging from 0.37 μM to 3.29 mM (Arya *et al.,* 2021; Fayeulle *et al.,* 2021; Kafali *et al.,* 2024). Beyond lipid peroxidation, vanillin was reported to retard protein peroxidation in rat liver mitochondria, form adducts with radicals, and exhibit potent reactive oxygen species (ROS) quenching ability (Al-Baqami and Hamza, 2021). Additionally, the compound inhibited the overproduction of advanced glycation end products (AGEs), which are implicated in oxidative stress–related pathologies (Alhadid *et al.,* 2022).

In vivo studies have corroborated these findings. For example, vanillin (150 mg/kg body weight) protected against metribuzin-induced oxidative stress in rats by reducing malondialdehyde (MDA) levels and enhancing the activities of antioxidant defense enzymes (Sefi *et al.,* 2019). Similarly, intraperitoneal administration of vanillin at 100 mg/kg mitigated potassium bromate-induced oxidative damage in mice, reducing protein and lipid peroxidation while improving antioxidant enzyme activities (Farag *et al.,* 2024). The compound also attenuated CCl_4-induced oxidative damage in rats, reducing protein carbonyl and MDA levels, restoring erythrocyte membrane enzyme activities (Ca^{2+}-ATPase and Na^+/K^+-ATPase), and preventing mitochondrial membrane damage (Arya *et al.*, 2021; Fayeulle *et al.*, 2021).

Vanillin also exhibits anti-inflammatory and analgesic effects. In vitro, it suppressed LPS-induced activation of NF-κB and down-regulated cyclooxygenase-2 (COX-2) expression in RAW 264.7 macrophages (Kafali *et al.*, 2024; Kamaly *et al.,* 2025), while also reducing nitric oxide (NO) production, inducible nitric oxide synthase (iNOS) activity, and MAPK signaling in microglial cells (Abbas *et al.*, 2022). Supporting these findings, in vivo studies showed that oral administration of vanillin (50–200 mg/kg body weight) reduced paw edema in carrageenan-induced inflammation in rats (Kumar *et al.,* 2025). Inhalation of the compound for 20 minutes in C57BL/6 mice suppressed pain responses in the hot plate test without affecting general behavior, indicating both anti-nociceptive and muscle relaxant properties (Ueno *et al.,* 2019).

CHAPTER THREE

MATERIALS AND METHODS

3.1 REAGENT / CHEMICALS

All reagents and chemicals were of analytical grade. They include potassium permanganate, distilled water, Na_2HPO_4, NaH_2PO_4, H_2SO_4, hydrogen peroxide, Na_2CO_3, $NaHCO_3$, EDTA-disodium, hydrochloric acid, adrenaline, pyrogallol, trichloroacetic acid, manganese chloride, vanillin, alcohol (50%, 70%, 90%, 100%), xylene, paraffin, formal saline, chloroform.

3.2 EQUIPMENT

Surgical latex glove, weighing balance, orogastric tube, measuring cylinder, conical flask volumetric flask, plastic cages, mortar and pestle, refrigerator, oven, sample bottles, water bath, paraffin dispenser, dissecting set, glass rods, rotary microtome, binocular microscope.

3.3 EXPERIMENTAL ANIMALS

The animals for this study were bred at the Animal House, Department of Anatomy, School of Basic Medical Sciences, College of Medical Sciences, University of Benin, Benin City, Edo State, Nigeria. The Wistar rats were kept in polypropylene cages at normal room temperature. The animals were fed with Chikun Feed Grower Mash (Olam Agri Holdings Pte Ltd., Lagos State, Nigeria) and had free access to water throughout the entire study period of twenty-eight days. The animals were weighed weekly before commencement and throughout the duration of the experiment using a digital weighing scale calibrated in grams and recorded to the nearest whole number. Protocols for this experiment were in accordance with the guide for the care and use of laboratory animals (National Research Council of the National Academics, 2011). Ethical approval for the study was obtained from the Research Ethics Committee, College of Medical Sciences, University of Benin, Benin City, Nigeria, with ethical approval number: **CMS/REC/2025/819.**

3.4 RESEARCH DESIGN

Forty-eight (48) adult Wistar rats weighing between 170g and 180g were used for this study. They were randomly assigned into six groups (A, B, C, D, E, and F) of eight rats each after acclimatization to animal house conditions for three weeks with free access to feed and water.

Group	Treatment
A	Control
B	10 mg/kg body weight of manganese chloride
C	20 mg/kg body weight of Vanillin + 10 mg/kg body weight of manganese chloride
D	40 mg/kg body weight of Vanillin + 10 mg/kg body weight of manganese chloride
E	20 mg/kg body weight of Vanillin
F	40 mg/kg body weight of Vanillin

Manganese chloride was administered via intra-peritoneal route, while Vanillin was administered orally. All administrations lasted for 28 days.

3.5 NEUROBEHAVIOURAL ASSESSMENTS

To assess the effects of treatments on neurobehavioural activities, various neurobehavioural assessment tests were carried out. These include; Open field, movement initiation, string and Step tests.

3.5.1 Novel Object Recognition (NOR) Test

The novel object recognition (NOR) test also known as the object recognition test (ORT) is a standard behavioural assay utilized to investigate many aspects of learning and memory in rodents (Lueptow, 2017). The NOR's key benefit over other rodent memory tests is that it takes advantage of rodents' innate inclination to seek out novelty. The test was performed as described by Enogieru and Omoruyi, (2022). The NORT was performed in a wooden open box apparatus (80 × 60 × 40 cm). The objects to be discriminated was of two different colours (yellow and pink), made up of painted wood, around 10 cm in height and heavy (so it will not be displaced by the animals during test). In addition, these objects had no genuine significance for the rats and were not associated with reinforcement.

3.5.2 Elevated-plus Maze (EPM) Test

According to Carobrez and Bertoglio (2005), the Elevated Plus Maze (EPM) is commonly employed to assess anxiety-like behavior in laboratory rodents, though it can also be utilized to evaluate cognitive function. The apparatus consists of two open arms (50 × 10 cm) and two closed arms of the same dimensions, with the closed arms enclosed by 30 cm high walls. These arms are arranged in a plus-shaped configuration and connected by a central platform (10 × 10 cm), with the entire maze elevated 60 cm above the ground. Each rat was placed at the center of the maze facing an open arm and allowed to explore freely for 5 minutes. During this period, transfer latency parameters was recorded. Transfer latency is defined as the time taken for the animal to move from the open arm into a closed arm upon initial placement in the maze, often interpreted as an index of cognitive function or exploratory motivation. An arm entry was recorded when all four paws of the animal (or at minimum, both hind paws) were fully within the arm. To prevent olfactory cues from affecting behavior, the maze was cleaned with 70% ethanol between trials. (de Figueiredo Cerqueira *et al*., 2023).

3.6 EVALUATION OF BRAIN WEIGHT

The rats were sacrificed with ketamine anesthesia (100 mg/kg), followed by cervical dislocation, once the neurobehavioral tests were finished. Rats' brains were removed from their skulls, blotted clean of blood, and instantly weighed using an electronic balance calibrated in milligrams and recorded to the nearest two decimal places. The relative brain weight was calculated as follows:

Relative brain weight = [absolute brain weight (g) / body weight of rat (g)] x 100

3.7 HIPPOCAMPAL OXIDATIVE STRESS PARAMETERS

The harvested and weighed brains were homogenized with acid-washed sand and PBS in a porcelain mortar and pestle after being washed twice in cold phosphate-buffered saline (PBS). Then the homogenate was centrifuged at 10,000 g for 15 minutes at 4 °C, while the supernatant was gathered to estimate the results of several biochemical experiments.

3.7.1 Estimation of Catalase (CAT) activity

This was determined by the method of Cohen *et al*. (1970). Catalase is present in nearly all animal, plant, and bacteria cells. It acts to prevent the accumulation of noxious H_2O_2 which is converted to O_2 and H_2O.

- ***Preparation of reagent:*** 0.01M $KMnO_4$ was prepared by dissolving 0.158g of $KMnO_4$ in 100 ml of distilled water. Phosphate buffer (pH 7.4); 0.426 of $NaHPO_4$ NaH_2PO_4 was weighed and dissolved in 100ml of distilled water. 6M H_2SO_4: 32.3ml of conc. H_2SO_4 was added to 66.7 ml of distilled water. 30Mm H_2O_2 solution: this was prepared by measuring 0.34 ml of 30% of H_2O_2 in 1001 ml of phosphate buffer.

- ***Procedure:*** To a known volume of supernatant, (0.5ml), 5.0ml of H_2O_2 was added. This was then mixed by inversion and allowed to stand for 30 minutes. The reaction was stopped by adding 6M H_2SO_2. The absorbance was taken at 480nm within 30-60 seconds against distilled water.

- ***Calculation:*** Activity = [OD / × min × Vt] / [M × V × L ×Y]

Where, OD= absorbance

L= light path =1cm

Vt = total volume of the reaction sample

M= molar extinction co-efficient of H2O2 (40/M/cm)

3.7.2 Estimation of Malondialdehyde (MDA) activity

Malondialdehyde was determined using the thiobarbituric acid assay (Buege and Aust, 1978). Malondialdehyde which is a product of lipid peroxidation reacts with thiobarbituric acid to give a red species.

- ***Preparation of reagent:*** Stock TCA-TCB-HCL was prepared by mixing 15g of trichloroacetic acid, 0.375g of thiobarbituric acid and 0.25N hydrochloric acid. This solution was mildly heated to assist in the dissolution of the thiobarbituric acid.
- ***Procedure:*** A volume of supernatant (1.0ml) was added to 2.0ml of TCA-TBA-HCL and mixed thoroughly. The solution was heated for 15 minutes in a boiling water bath. After cooling, the flocculent precipitate was removed by centrifuging at 1000g for 10 minutes. The absorbance was determined at 535mn against a blank. The concentration MDA was determined using the formula:

$$\text{MDA (unit/mg protein)} = [(A \times Vt \times 1000)] / [(M \times V \times l \times Y)]$$

Where, A = absorbance of sample test at 535nm

Vt= total volume of the reaction = 3ml

M = molar extinction co-efficient of product= 1.56 × 105/mcm

l = light path= 1cm

V= volume of tissue extract used = 1ml

Y = mg tissue in the volume of sample used

3.7.3 Estimation of Glutathione Peroxidase (GPx) activity

This was determined by the method of Nyman (1959). This was based on the oxidation of pyrogallol to purpurogallin by peroxidase activity, resulting in a deep brown colour disposition, read at 430nm.

- ***Preparation of reagent:*** Pyrogallol (20mM): 0.2552g of pyrogallol was dissolved in 100ml of distilled water.

- ***Procedure:*** To an aliquot of plasma (0.2ml), 2.5ml of phosphate buffer, 2.5ml of H_2O_2, 1.5ml of distilled water and 2.5ml of pyrogallol were added. The reaction was allowed to stand for 30 minutes at room temperature. A deep brown color was formed which was read at 420nm.
- ***Calculation:*** Activity = $[OD/Min \times VtDf]$ / $[E \times Vs \times Y]$

  OD = Absorbance of test

  Vt = Total volume of reaction of reaction mixture

  Df = Dilution factor = l

  E = Molar extinction coefficient (12/M/cm)

  Vs= volume of sample

  Y = mg of protein used

3.7.4 Estimation of Superoxide Dismutase (SOD)

This was determined according to the method of Misra and Fridovich (1972)

- ***Principle:*** Adrenaline undergoes autoxidation rapidly to adrenochrome whose concentration can be determined at 420 nm with the aid of a spectrophotometer. The auto-oxidation of adrenaline depends on the presence of superoxide anions. Superoxide dismutase inhibited the auto-oxidation of adrenaline by catalyzing the breakdown of superoxide anion. The degree of inhibition reflected the activity of SOD which was determined at 420 nm.
- ***Preparation of reagents:*** Carbonate buffer (0.05 M) pH 10.2 was prepared by dissolving 0.2014 g of Na_2CO_3. 0.2604 g of $NaHCO_3$ and 0.0372 g of EDTA in 100 ml of distilled water. Hydrochloric acid (0.005 M) was prepared by adding 0.044 concentrated HCl to 99.96 ml of distilled water. Adrenaline solution (0.3 mM) was prepared by dissolving 0.01098 g of Adrenaline in 100 ml of 0.005 M HCl solution.
- ***Procedure:*** A supernatant volume of 0.2 ml was mixed with 2.5 ml of carbonate buffer and 0.3 ml of adrenaline solution, and 0.2 ml of distilled water was mixed with 2.5 m of

carbonate buffer and 0.3 ml adrenaline as reference sample. These were mixed and absorbance read at 420 nm.

$$\% \text{ inhibition} = [(\text{O.D test} - \text{O.D ref}) \times 100] / \text{O.}D\ test$$

Enzyme activity was calculated thus:

$$\text{SOD activity (Unit/ mg protein)} = [\%\ inhibition] / [50 \times Y]$$

Where Y = mg of protein in the volume of sample used.

3.8 HISTOLOGY OF THE HIPPOCAMPUS

Briefly, the excised hippocampal tissues were fixed in 10% buffered formal saline. The paraffin wax embedded method of Drury and Wallington (1980) was used to prepare the tissues. They were each dehydrated for an hour at room temperature using ethanol concentrations of 70%, 90%, absolute ethanol I, and absolute ethanol II. Two xylene changes at room temperature, lasting an hour each, was used to remove the dehydrated tissue. The tissues were then soaked in two separate batches of molten paraffin wax for one hour each at 60 degrees Celsius before being embedded in multi-block paraffin wax molds. The paraffin-blocked tissues were then cut into smaller pieces and put on a wooden chuck for rotary microtome sectioning. A rotary microtome was used to slice the tissue blocks into sections that were 5m thick. To spread the parts' folded ribbons, the sections were placed in a water bath at 40 degrees Celsius. These pieces were fixed to a fresh, spotless glass slide. To increase the adherence of the sections to the slides, these were dried at 40°C using a slide drier.

3.9 HEMATOXYLIN AND EOSIN STAINING PROCEDURES

Tissue sections were deparaffinized in two changes of xylene for two minutes in each change and passed through two changes of absolute alcohol for four minutes each. They were hydrated using a series of descending grades of alcohol until water was used. Procedures of Haematoxylin and Eosin adopted on the sections was done as described by Drury and

Wallington (1980). The sections were dewaxed in two changes of xylene for two minutes in each change after which they were then rehydrated in descending grades of alcohol (absolute II, absolute I, 95%, 90%, 70% and 50% ethanol) for two minutes each. Afterwards, it was then rinsed in distilled water for three minutes and stained in hematoxylin for 15-20 minutes. The excess hematoxylin stain was removed by rinsing well in running tap water for two to three minutes (sections were examined microscopically at this stage to confirm sufficient degree of staining). It was then differentiated in acid alcohol (0.5% HCL in 70% ethanol) for two to three minutes and rinsed well in running water for 10-15 minutes before counterstaining in 1% aqueous eosin for two to four minutes. Excess stains were washed off in running water and examined under a microscope and was then dehydrated rapidly in ascending grades of ethanol (50% through absolute ethanol), cleared in xylene and mounted in a synthetic resin medium (DPX).

3.10 PHOTOMICROGRAPHY

A binocular microscope equipped with an Omax 9.0MP USB Digital Microscope Camera (manufactured in Korea) was used to take pictures of the treated slides. The camera had a 0.5X reduction lens and a 9 megapixel (3488 x 2616 pixel) high quality color digital camera. The use of 4 and 10 objective lenses was used to produce a panoramic image of the slides.

3.11 STATISTICAL ANALYSIS

Data was analyzed using GraphPad Prism statistical package (version 9). Statistical significance (P<0.05) was determined by means of analysis of variance (ANOVA), followed by Tukey's multiple comparison post-hoc test. Results were presented as mean ± standard error of mean (mean ± SEM).

CHAPTER FOUR

RESULTS

4.1 EFFECT OF TREATMENT ON BODY AND BRAIN WEIGHTS

Figure 4.1 and 4.2 shows the initial and final body weights across experimental groups. There was no significant difference ($p>0.05$) in the initial body weight and final body weight of rats across the treated groups when compared to control.

Figure 4.3 shows the weight change of rats across experimental groups. There was a significant decrease ($p<0.05$) observed in $MnCl_2$ only group when compared to control. However, a significant increase ($p<0.05$) was observed in the $MnCl_2$-exposed rats pretreated with vanillin when compared to the $MnCl_2$ only group.

Figure 4.4 shows the whole brain weights of rats across experimental groups. There was a significant decrease ($p<0.05$) observed in $MnCl_2$ only group when compared to control. However, a significant increase ($p<0.05$) was observed in the $MnCl_2$-exposed rats pretreated with 20 mg/kg vanillin when compared to the $MnCl_2$ only group.

Figure 4.5 shows the relative brain weights of rats across experimental groups. There was no significant change ($p>0.05$) in the relative brain weight of rats across the treated groups when compared to control.

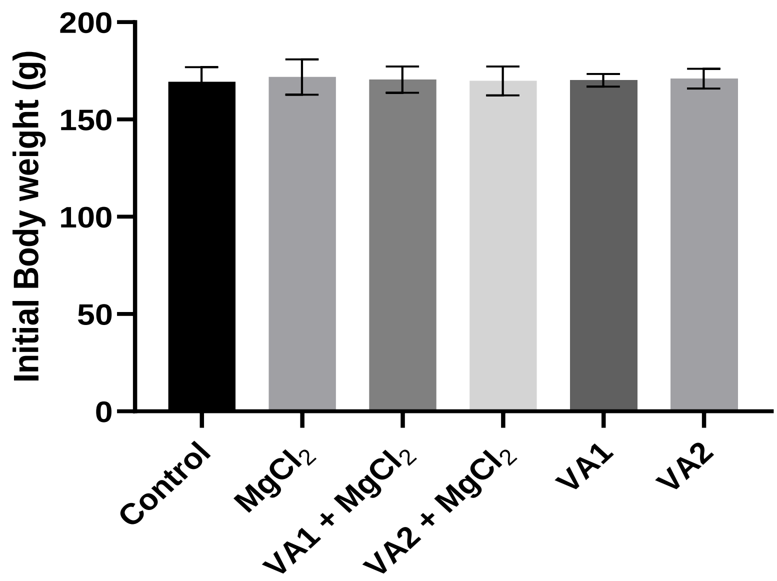

Figure 4.1: Initial body weight across experimental groups.

Values are given as mean ± SEM of each group.

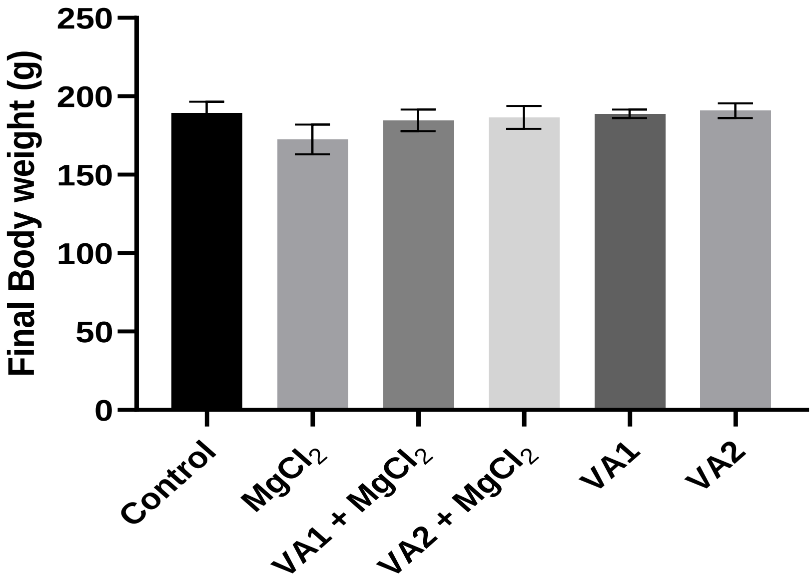

Figure 4.2: Final body weight across experimental groups.

Values are given as mean ± SEM of each group.

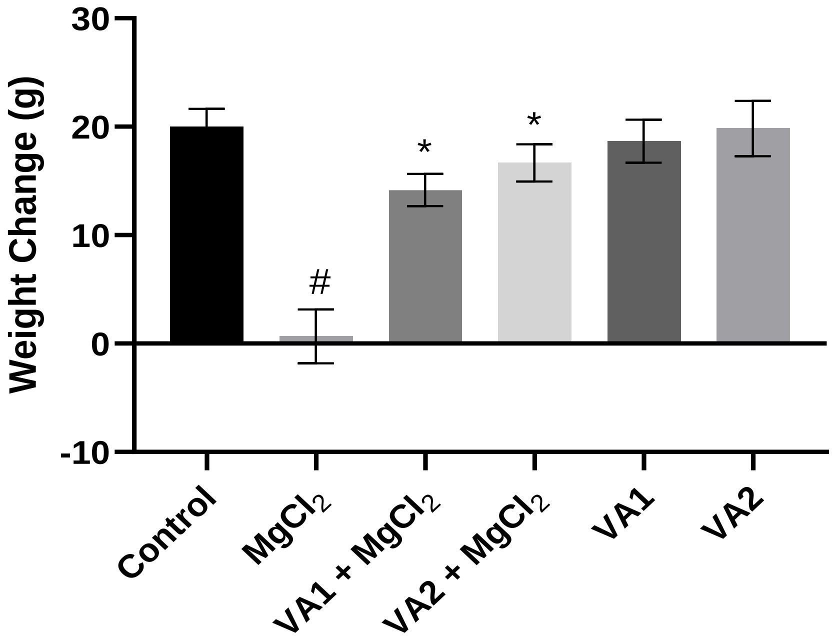

Figure 4.3: Weight change across experimental groups.

Values are given as mean ± SEM of each group. # $p<0.05$ compared with the control group; * $p<0.05$ compared with $MnCl_2$ group

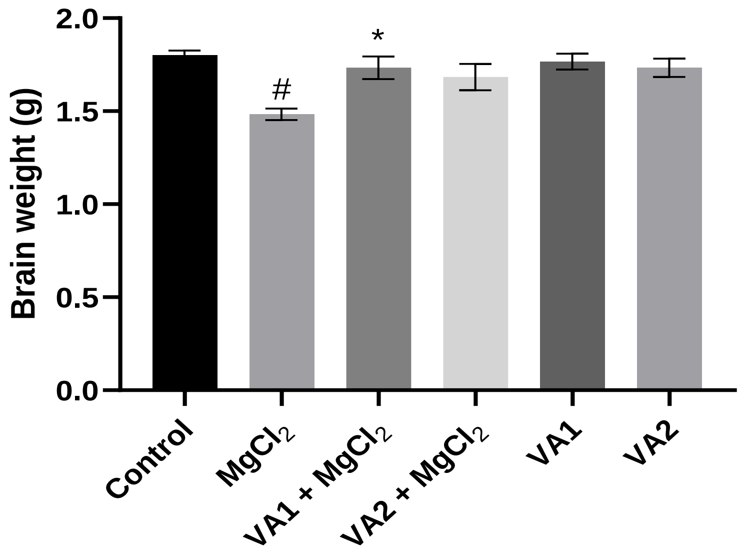

Figure 4.4: Brain weight across experimental groups.

Values are given as mean ± SEM of each group. # $p<0.05$ compared with the control group; * $p<0.05$ compared with $MnCl_2$ group

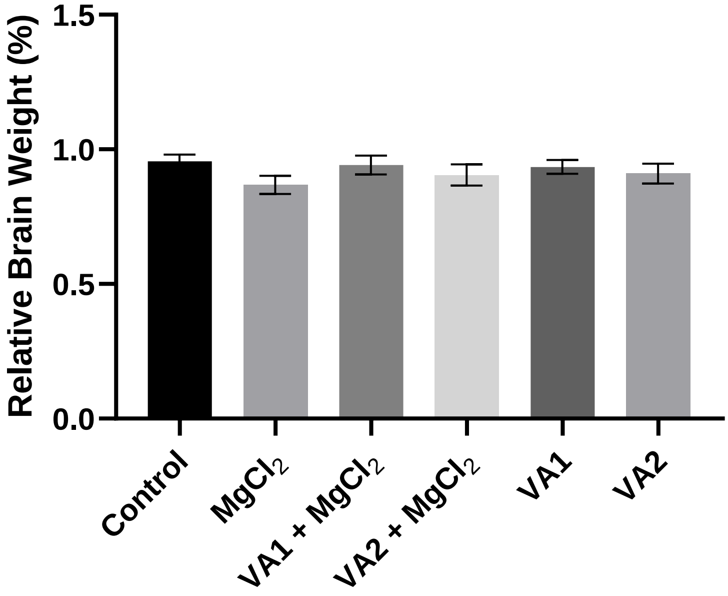

Figure 4.5: Relative brain weight across experimental groups.

Values are given as mean ± SEM of each group.

4.2 EFFECT OF TREATMENT ON NEUROBEHAVIOURAL ACTIVITY

4.2.1 Novel Object Recognition (NOR)

Figure 4.6 shows the discrimination index across experimental groups. There was a significant decrease ($p<0.05$) in the discrimination index in rats treated with $MnCl_2$ only when compared to control. However, there was a significant increase ($p<0.05$) in $MnCl_2$-exposed rats pretreated with vanillin when compared to $MnCl_2$ only group.

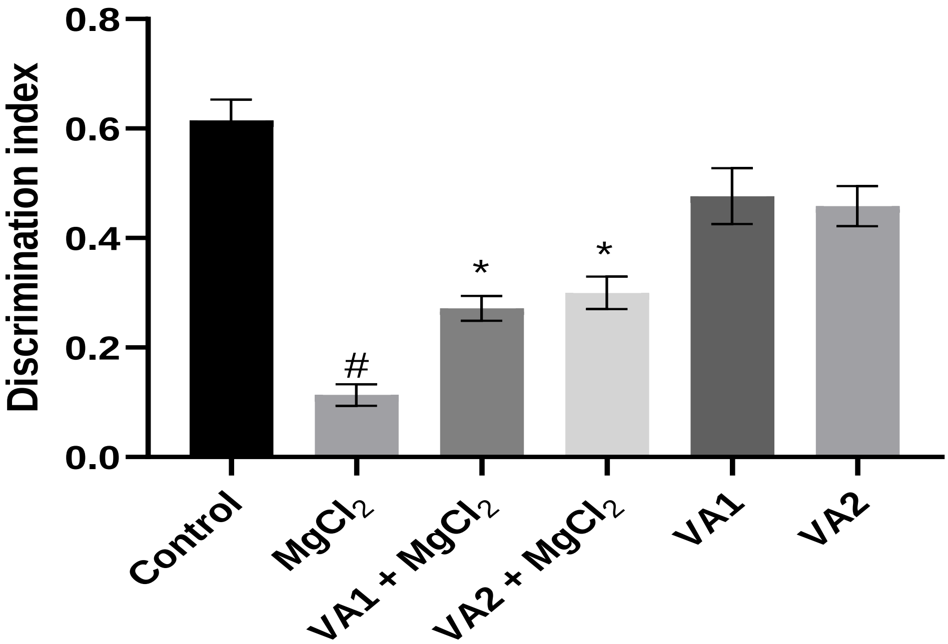

Figure 4.6: discrimination index of control and treatment groups after 28 days.

Values are given as mean ± SEM of each group. # $p<0.05$ compared with the control group; * p<0.05 compared with $MnCl_2$ group.

4.2.2 Elevated Plus Maze (EPM)

Figure 4.7 shows the transfer latency across the experimental groups. A significant increase ($p<0.05$) in the transfer latency was observed in rats treated with $MnCl_2$ only when compared to control. However, there was a significant decrease ($p<0.05$) in the transfer latency of $MnCl_2$-exposed rats pretreated with vanillin when compared to $MnCl_2$ only group.

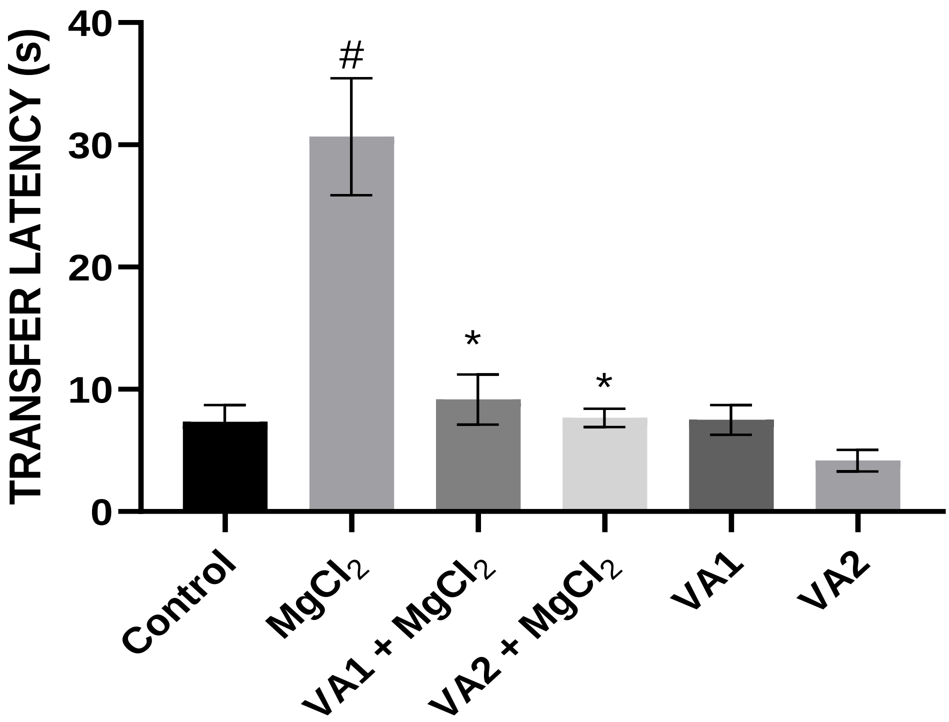

Figure 4.7: Transfer Latency of control and treatment groups after 28 days.

Values are given as mean ± SEM of each group. # $p<0.05$ compared with the control group; * p<0.05 compared with $MnCl_2$ group.

4.3 EFFECT OF TREATMENT ON OXIDATIVE STRESS

Figure 4.8 shows hippocampal Superoxide dismutase (SOD) activity across experimental groups. Rats treated with $MnCl_2$ only showed a significant decrease ($p<0.05$) in SOD activity when compared to control. However, there was a significant increase ($p<0.05$) in SOD activity in $MnCl_2$-exposed rats pretreated with vanillin when compared to $MnCl_2$ only group.

Figure 4.9 shows hippocampal catalase (CAT) activity across experimental groups. There was a significant decrease ($p<0.05$) in the CAT activity in rats treated with $MnCl_2$ only when compared to control. However, there were a significant increase ($p<0.05$) in CAT activity in $MnCl_2$-exposed rats pretreated with vanillin when compared to $MnCl_2$ only group.

Figure 4.10 shows hippocampal glutathione peroxidase (GPx) activity across experimental groups. There was a significant decrease ($p<0.05$) in GPx activity in rats treated with $MnCl_2$ only when compared to control. However, there were a significant increase ($p<0.05$) in GPx activity in $MnCl_2$-exposed rats pretreated with vanillin when compared to $MnCl_2$ only group.

Figure 4.11 shows glutathione (GSH) concentration in the hippocampus across experimental groups. Rats treated with $MnCl_2$ only showed a significant decrease ($p<0.05$) in GSH concentration when compared to control. However, there were a significant increase ($p<0.05$) in GSH concentration in $MnCl_2$-exposed rats pretreated with vanillin when compared to $MnCl_2$ only group.

Figure 4.12 shows hippocampal Malondialdehyde (MDA) concentration across experimental groups. There was a significant increase ($p<0.05$) in MDA concentration in rats treated with $MnCl_2$ only when compared to control. However, there were a significant decrease ($p<0.05$) in MDA concentration in the $MnCl_2$-exposed rats pretreated with vanillin when compared to $MnCl_2$ only group.

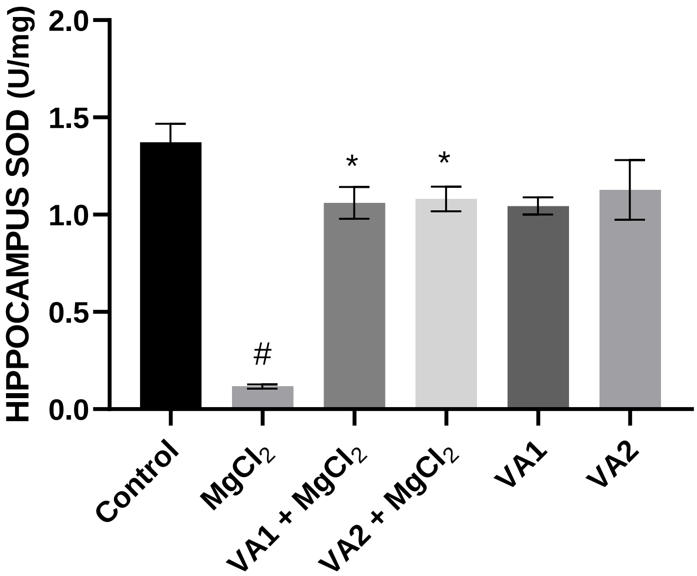

Figure 4.8: Hippocampus SOD activity of control and treatment groups after 28 days.

Values are given as mean ± SEM of each group. # p<0.05 compared with the control group;

* *p*<0.05 compared with $MnCl_2$ group.

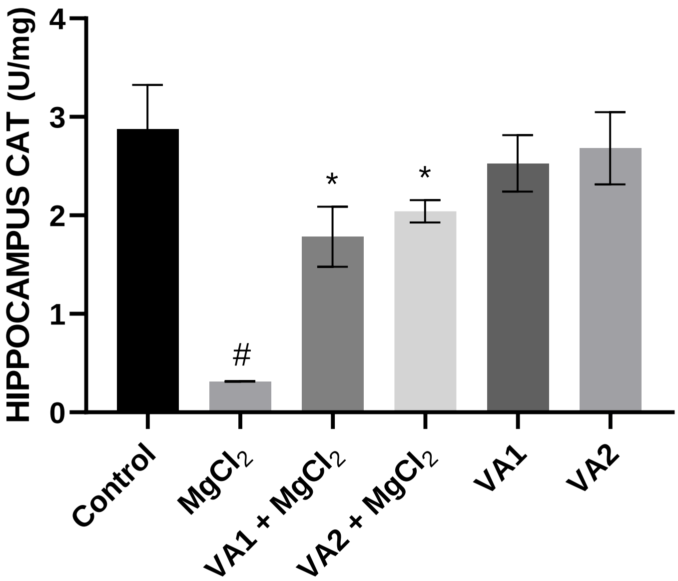

Figure 4.9: Hippocampus CAT activity of control and treatment groups after 28 days.

Values are given as mean ± SEM of each group. # p<0.05 compared with the control group;

* *p*<0.05 compared with $MnCl_2$ group.

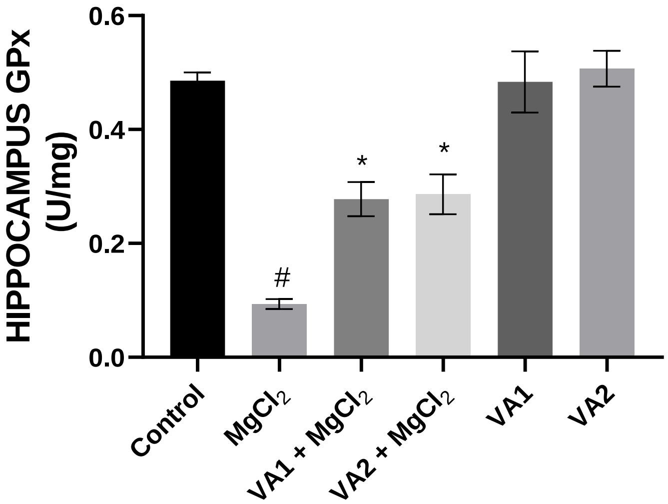

Figure 4.10: Hippocampus GPx activity of control and treatment groups after 28 days.

Values are given as mean ± SEM of each group. # $p<0.05$ compared with the control group;

* $p<0.05$ compared with $MnCl_2$ group.

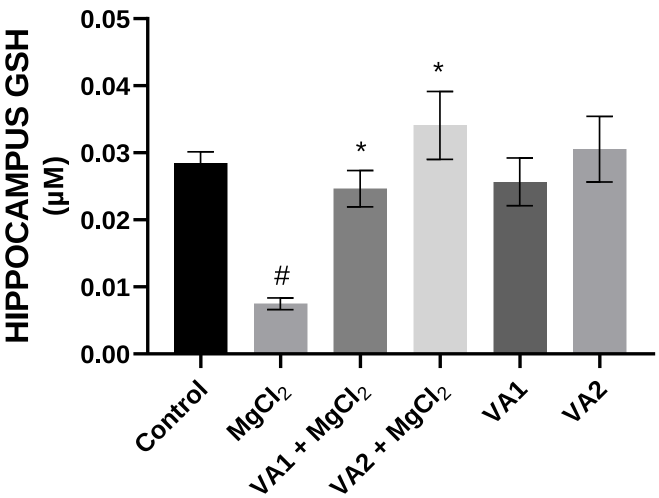

Figure 4.11: Hippocampus GSH levels of control and treatment groups after 28 days.

Values are given as mean ± SEM of each group. # $p<0.05$ compared with the control group;

* $p<0.05$ compared with $MnCl_2$ group.

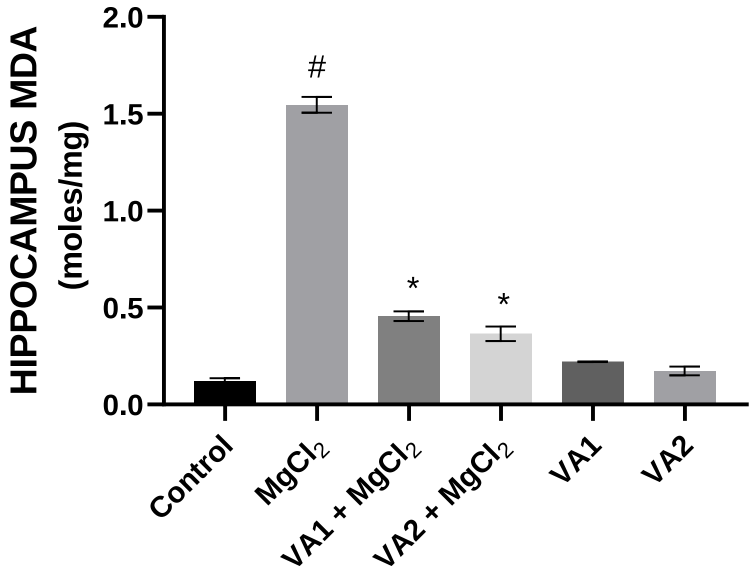

Figure 4.12: Hippocampus MDA concentration of control and treatment groups after 28 days. Values are given as mean ± SEM of each group. # p<0.05 compared with the control group; * *p*<0.05 compared with $MnCl_2$ group.

4.4 EFFECT OF TREATMENT ON THE HISTOLOGY OF THE HIPPOCAMPUS

Plate 4.1-4.6 show the histology of the hippocampus (CA1) of rats across experimental groups. Plate 4.1 shows the histology of rats in control group with normal structure of pyramidal cells. Plate 4.2 shows the hippocampal histology of $MnCl_2$ only treated rats showing atrophy and vacuolated pyramidal cells and astrocytes, also observed is general distortion of hippocampal architecture. The hippocampus of $MnCl_2$-exposed rats pretreated with vanillin (Plate 4.3 and 4.4) shows relatively normal histological structures. Plates 4.5 and 4.6 shows the hippocampal histology of rats treated with vanillin only, showing relatively normal hippocampal features.

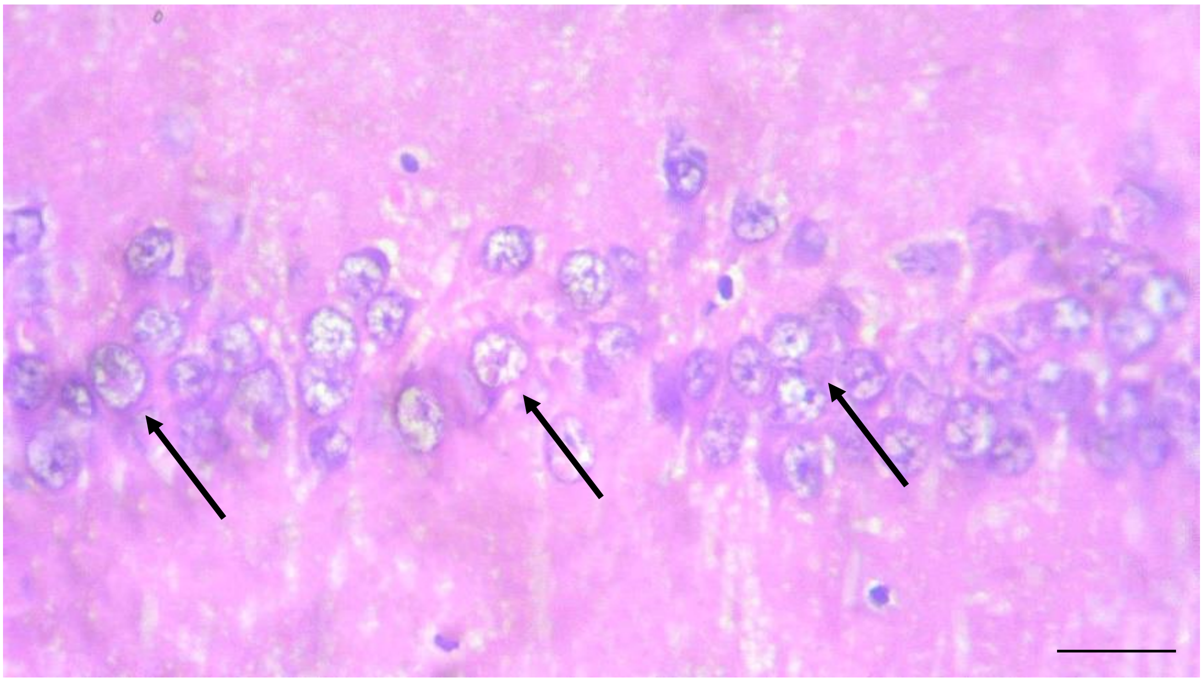

Plate 4.1: Representative histology of the hippocampus CA1 in control showing normal structure of pyramidal cells (arrows). (H&E; Scale bar: 25µm)

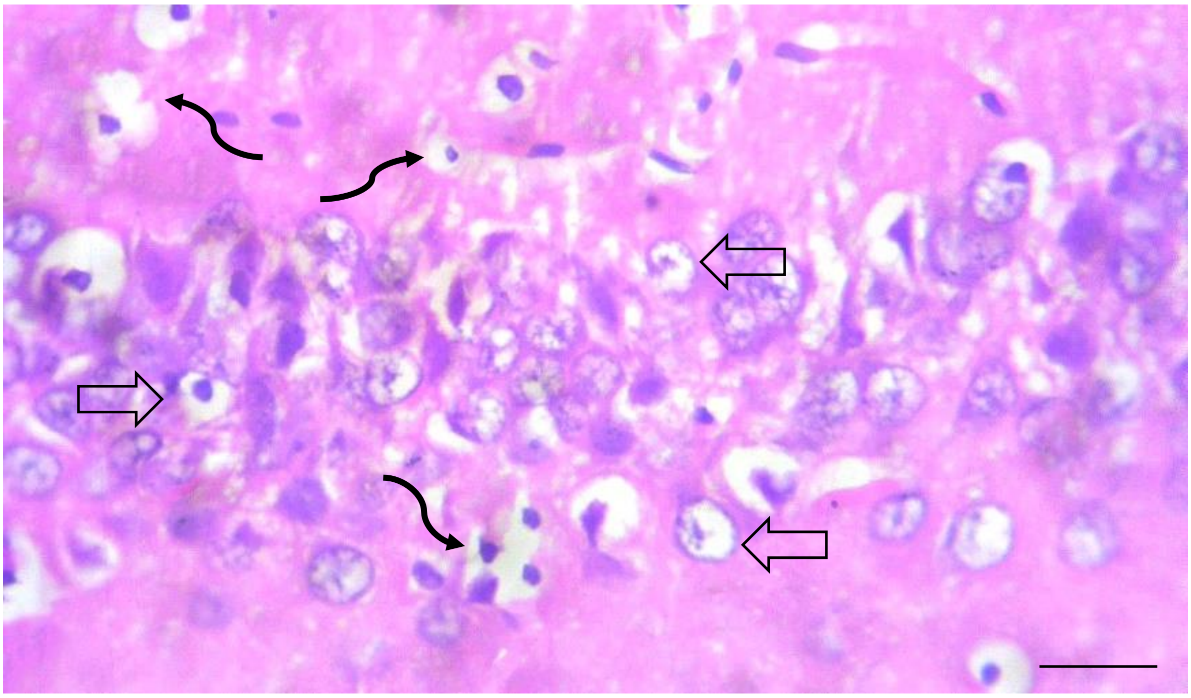

Plate 4.2: Representative histology of the hippocampus CA1 in $MnCl_2$-treated rats showing atrophy and vacuolated pyramidal cells (double arrows) and astrocytes (curved arrows); Also observed is general distortion of hippocampal architecture. (H&E; Scale bar: 25µm).

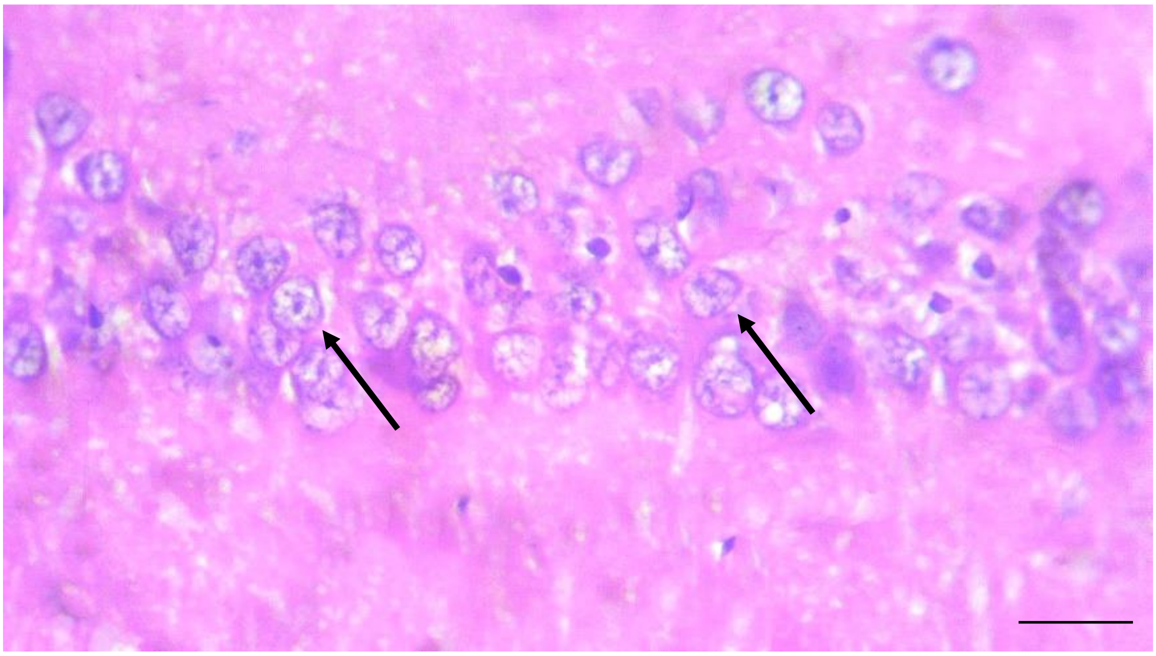

Plate 4.3: Representative histology of the hippocampus CA1 in $MnCl_2$-treated rats pre-treated with vanillin (20 mg/kg) showing Relatively normal histological structure of the hippocampus observed. (H&E; Scale bar: 25µm)

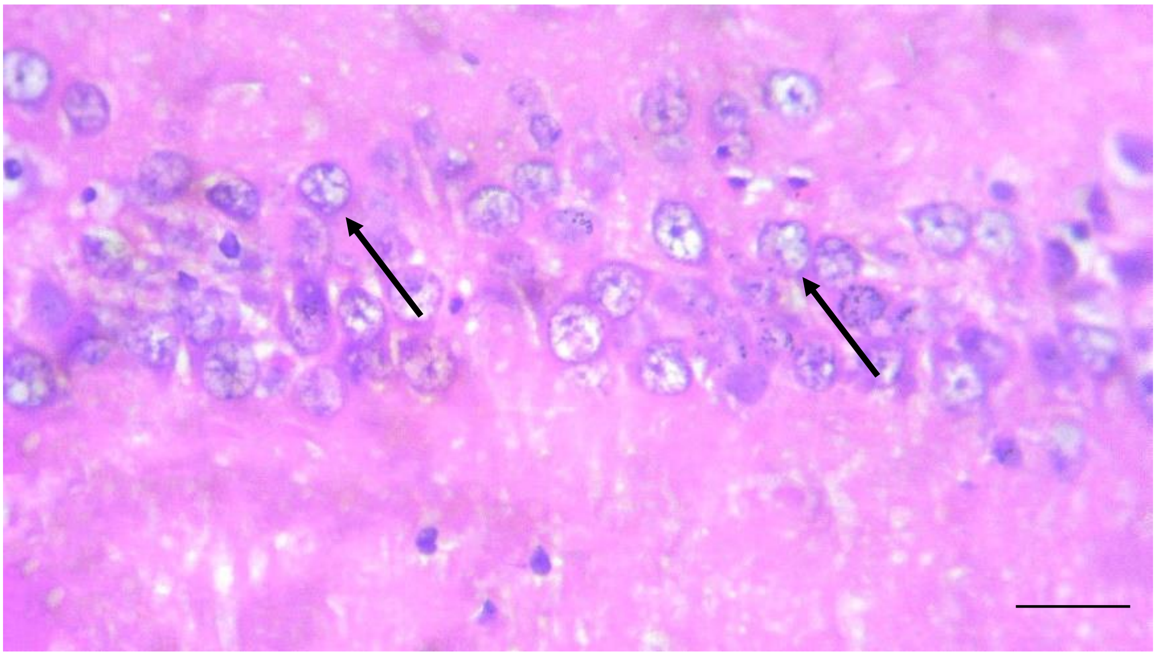

Plate 4.4: Representative histology of the hippocampus CA1 in $MnCl_2$-treated rats pre-treated with vanillin (40 mg/kg) showing Relatively normal histological structure of the hippocampus observed. (H&E; Scale bar: 25µm)

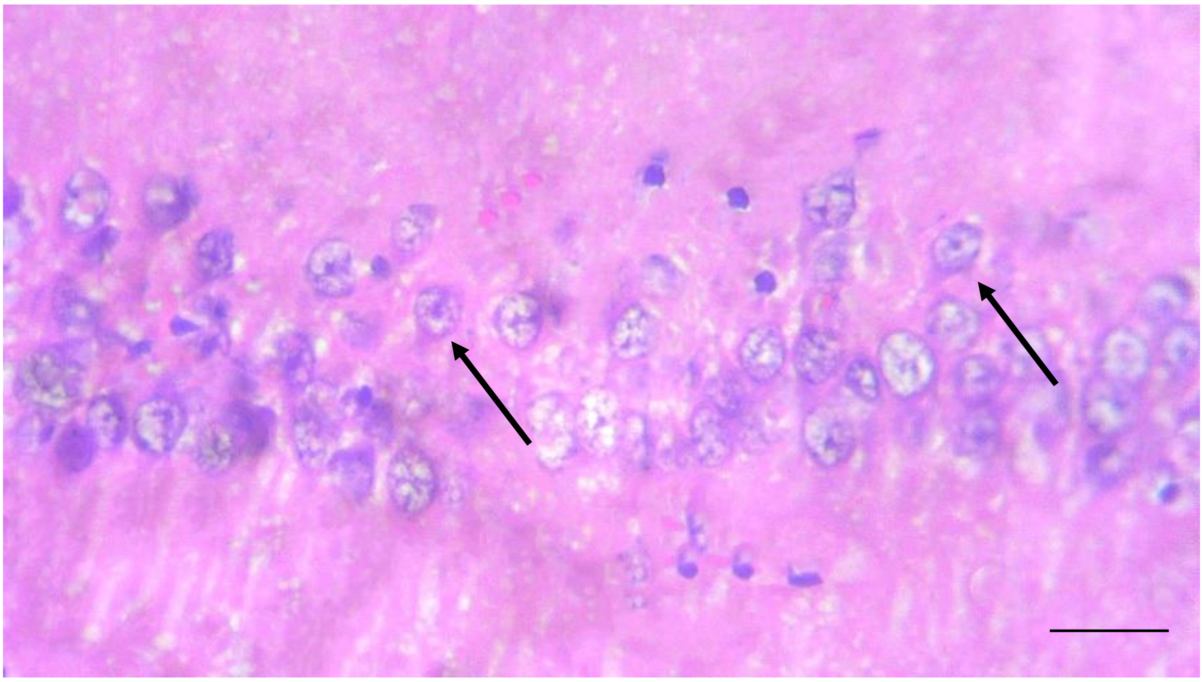

Plate 4.5: Representative histology of the hippocampus CA1 in vanillin (20 mg/kg) showing showing Relatively normal histological structure of the hippocampus observed. (H&E; Scale bar: 25µm)

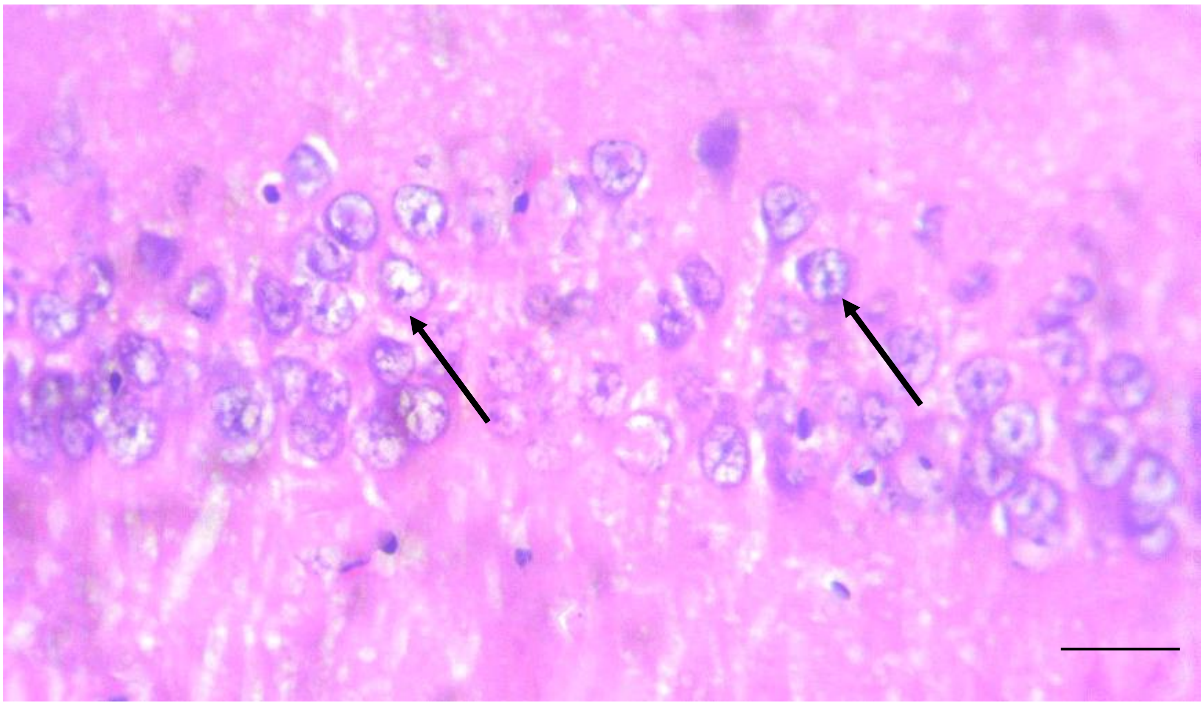

Plate 4.6: Representative histology of the hippocampus CA1 in vanillin (40 mg/kg) showing Relatively normal histological structure of the hippocampus observed. (H&E; Scale bar: 25µm)

CHAPTER FIVE

DISCUSSION, CONCLUSION AND RECOMMENDATION

5.1 DISCUSSION

Exposure to manganese chloride ($MnCl_2$) produced measurable physiological effects reflected in alterations in body and brain weights. The absence of significant variation in initial and final body weights across the treatment groups suggests that short-term exposure did not drastically affect general somatic growth or feeding behaviour (McGough and Jardine, 2017; Jomova *et al*., 2025). However, the reduced weight change observed in the $MnCl_2$-only group indicates systemic toxicity and possible metabolic stress induced by excessive manganese accumulation (McGough and Jardine, 2017). Manganese is known to disrupt mitochondrial function and impair energy metabolism, which can manifest as reduced weight gain (Li and Yang, 2018). Interestingly, vanillin pre-treatment mitigated these effects, resulting in a significant improvement in weight change relative to the $MnCl_2$-only group. This finding supports the antioxidant and protective role of vanillin in reducing manganese-induced metabolic stress (Bezerra-Filho *et al*., 2019). Similarly, the reduction in whole brain weight observed in $MnCl_2$-exposed rats is consistent with earlier reports that manganese neurotoxicity leads to neuronal loss and brain tissue atrophy, particularly in cortical and hippocampal regions (Harischandra *et al*., 2019; Tarnacka *et al*., 2021). The restoration of brain weight in vanillin-treated groups suggests that the compound may preserve neuronal integrity and prevent neurodegenerative changes (Kafali *et al*., 2024). The relative brain weight, however, remained unchanged across all groups, implying that brain-to-body ratio was proportionally maintained despite absolute weight fluctuations.

Cognitive and emotional behaviours are critically dependent on the functional integrity of the hippocampus, prefrontal cortex, and amygdala—regions highly susceptible to heavy metal-induced oxidative and inflammatory stress (Lupien *et al*., 2018). In this study, behavioural paradigms such as the Novel Object Recognition (NOR) and Elevated Plus Maze (EPM) were employed to assess memory performance, learning ability, and anxiety-related responses following manganese chloride ($MnCl_2$) exposure. These tasks are well-validated tools in behavioural neuroscience for evaluating higher-order cognitive and affective processes in rodent models (Sakhaje *et al*., 2020). In the Novel Object Recognition (NOR) test, a significant decline in discrimination index was observed in the $MnCl_2$-only group, indicating impaired recognition memory and deficits in cognitive flexibility. The NOR test relies on the rodent's natural tendency to explore novel stimuli more than familiar ones; thus, reduced discrimination suggests failure in object recognition and memory retrieval processes (Enogieru and Omoruyi, 2022). These impairments point to compromised hippocampal and cortical circuitry, particularly within the perirhinal and entorhinal cortices that mediate recognition memory. The hippocampus plays a pivotal role in encoding, consolidating, and retrieving memory traces; its dysfunction is strongly associated with deficits in both short-term and long-term recognition tasks (Gliebus *et al*., 2018; Adedayo *et al*., 2023). Mechanistically, the observed cognitive deficits are consistent with reports that Mn exposure disrupts synaptic plasticity, alters long-term potentiation (LTP), and impairs cholinergic and glutamatergic neurotransmission within the hippocampus (Ma *et al*., 2020; Guan *et al*., 2022). Manganese has been shown to promote oxidative stress, mitochondrial dysfunction, and neuroinflammation, all of which contribute to synaptic degeneration and neuronal loss (Harischandra *et al*., 2019; Mezzaroba *et al*., 2019). These pathological events collectively impair the neurochemical substrates required for learning and memory. The decline in discrimination index therefore reflects a functional manifestation of oxidative and synaptic disturbances in hippocampal neurons resulting from Mn-induced neurotoxicity (Harischandra *et al*., 2019; Tarnacka *et al*., 2021). Conversely, vanillin pre-treatment produced a significant improvement in the discrimination index, suggesting restoration of cognitive performance and recognition ability. This improvement may be attributed to vanillin's ability to enhance cholinergic neurotransmission and reduce oxidative stress, thereby preserving neuronal integrity and synaptic plasticity (Kafali *et al*., 2024). Vanillin's phenolic hydroxyl group confers potent free radical scavenging properties, enabling it to neutralize reactive oxygen species and inhibit lipid peroxidation within the hippocampus (Salau *et al*., 2020). Additionally, vanillin may upregulate antioxidant enzymes and improve acetylcholine availability, enhancing cognitive processes mediated by hippocampal and cortical networks (Anand *et al*., 2022).

The Elevated Plus Maze (EPM) test was employed to assess learning and memory performance, processes that are critically regulated by the hippocampus, amygdala, and prefrontal cortex (Lechin *et al*., 2020). Transfer latency—the time taken by a rat to move from the open arm to an enclosed arm—is used as an index of memory retention. $MnCl_2$-exposed rats exhibited prolonged transfer latency, indicating impaired learning and memory consolidation. This delay suggests that manganese exposure disrupts the neural circuits responsible for spatial and emotional memory processing. The EPM has been validated as a reliable tool for evaluating hippocampal-dependent memory, as decreased latency during subsequent trials reflects memory retention of the previous experience (De Brouwer *et al*., 2019). The observed $MnCl_2$-induced memory deficits may result from oxidative stress, mitochondrial dysfunction, and altered neurotransmitter activity within the hippocampus and prefrontal cortex, leading to synaptic instability and reduced neuroplasticity (Strasser *et al*., 2019; Sviridova *et al*., 2025). In contrast, vanillin pre-treatment significantly shortened transfer latency, suggesting enhanced learning ability and improved memory retention. The cognitive-protective effect of vanillin could be attributed to its antioxidant and anti-inflammatory properties, which preserve neuronal integrity, modulate cholinergic and glutamatergic signaling, and promote hippocampal synaptic plasticity (Iannuzzi *et al*., 2023; Farzan *et al*., 2023).

Exposure to $MnCl_2$ markedly suppressed hippocampal activities of superoxide dismutase (SOD), catalase (CAT), and glutathione peroxidase (GPx), along with a significant depletion of reduced glutathione (GSH) levels, while simultaneously elevating malondialdehyde (MDA) concentration. These alterations reflect an overwhelmed antioxidant defense system unable to neutralize excessive free radicals generated by Mn accumulation (Chandra and Roychoudhury, 2020; Engwa *et al*., 2022). Manganese readily participates in Fenton-like reactions that yield reactive oxygen species (ROS), particularly superoxide anions and hydroxyl radicals, leading to oxidative modifications of lipids, proteins, and nucleic acids within vulnerable hippocampal neurons (Timme-Laragy *et al*., 2024; Cao *et al*., 2025). Such disturbances in redox homeostasis compromise mitochondrial membrane potential, disrupt ATP synthesis, and promote cytochrome c release, thereby initiating caspase-dependent apoptotic cascades (Cao *et al*., 2025). The observed increase in MDA, a product of lipid peroxidation, further confirms structural damage to neuronal membranes and myelin lipids, which impairs synaptic transmission and cognitive processing (Petrovic *et al*., 2020). These biochemical alterations are consistent with previous reports that chronic Mn exposure induces neurodegeneration through oxidative stress-mediated pathways, affecting hippocampal and cortical neurons (Cheng *et al*., 2023; Ahmed *et al*., 2025). Conversely, pre-treatment with vanillin significantly enhanced the activities of SOD, CAT, and GPx and restored GSH levels toward normal, alongside a concomitant decline in MDA concentration. This antioxidant restoration highlights vanillin's ability to re-establish redox equilibrium by scavenging ROS and strengthening the endogenous antioxidant defense network. The phenolic hydroxyl group in vanillin's aromatic structure enables direct hydrogen donation to reactive radicals, interrupting lipid peroxidation chain reactions (More *et al*., 2021; Valgimigli *et al*., 2023). These findings correspond with earlier studies demonstrating that natural phenolics protect the hippocampus from oxidative and inflammatory insults by preserving mitochondrial function and inhibiting apoptotic signalling (Naoi *et al*., 2019; Rojas-García *et al*., 2023).

The hippocampus is highly vulnerable to oxidative injury and heavy metal neurotoxicity due to its dense synaptic networks and critical role in learning and memory (Cheng *et al*., 2023; Ahmed *et al*., 2025). Histological evaluation of the CA1 region in the $MnCl_2$-only group revealed degenerative changes such as neuronal atrophy, vacuolated pyramidal cells, and astrocytic proliferation—features consistent with oxidative damage and neuroinflammation (Ogunro and Olasehinde, 2024). The disruption of hippocampal architecture observed indicates loss of neuronal integrity and potential impairment of cognitive function. Conversely, rats pre-treated with vanillin exhibited well-preserved hippocampal morphology, with intact pyramidal layers and minimal degenerative alterations. This preservation of cytoarchitecture reflects the neuroprotective potential of vanillin in preventing Mn-induced hippocampal degeneration. Its action may involve free radical scavenging, stabilization of neuronal membranes, and suppression of pro-inflammatory cytokines (Iannuzzi *et al*., 2023; Kafali *et al*., 2024).

5.2 CONCLUSION

Results from this study showed that Vanillin protects against manganese chloride-induced hippocampal toxicity in Wistar rats. These findings suggest that Vanillin may serve as a potential therapeutic candidate in mitigating manganese chloride associated cognitive impairments.

5.3 RECOMMENDATION

Further studies should investigate its molecular mechanisms of action, long-term safety profile, and potential synergistic effects with other antioxidants in both experimental and clinical contexts. It would be beneficial to compare vanillin’s efficacy with other natural antioxidants or polyphenols to establish its relative potency and synergistic potential. Considering its safety and bioavailability, vanillin could be explored as a dietary or adjunct therapeutic intervention against occupational or environmental manganese exposure in humans.

REFERENCES

Aaseth, J. O., & Nurchi, V. M. (2022). Chelation Combination—A Strategy to Mitigate the Neurotoxicity of Manganese, Iron, and Copper?. *Biomolecules*, *12*(11), 1713.

Abbas, A., Mehmood, M. H. H., Siddique, R., & malik Kamran, A. A. (2022). Evaluation of the wound healing, anti-inflammatory, and antimicrobial activity of isovanillin by using an animal model.

Abdelmonem, M., Al-Mokaddem, A. K., & Zakaria, M. Y. (2025). TPGS-Functionalized Nanocarriers with improved flavonoid oral bioavailability and therapeutic Action: Pharmacokinetic and Mechanistic Insights in Diabetes-Induced Retinopathy. *European Journal of Pharmaceutics and Biopharmaceutics*, 114851.

Adedayo, L., Ojo, G., Umanah, S., & Bamidele, O. (2023). Hippocampus: Its Role in Relational. *Hippocampus: More than Just Memory*, 19.

Afolabi, O. B., Olasehinde, O. R., Olaoye, O. A., Jaiyesimi, K. F., Ekakitie, I. L., & Oloyede, O. I. (2023). Nephroprotective effects of caffeine, vanillin, and their combination against experimental ALCL3-induced renal toxicity in adult male wistar rats. *Biochemistry Research International*, *2023*(1), 6615863.

Agarwal, N., & Carare, R. O. (2021). Cerebral vessels: an overview of anatomy, physiology, and role in the drainage of fluids and solutes. Frontiers in neurology, 11, 611485.

Ahmed, G., Rahaman, M. S., Perez, E., & Khan, K. M. (2025). Associations of Environmental Exposure to Arsenic, Manganese, Lead, and Cadmium with Alzheimer's Disease: A Review of Recent Evidence from Mechanistic Studies. *Journal of Xenobiotics*, *15*(2), 47.

Alamri, E. S., El Rabey, H. A., Alzahrani, O. R., Almutairi, F. M., Attia, E. S., Bayomy, H. M., Albalwi, R.A., & Rezk, S. M. (2022). Enhancement of the protective activity of vanillic acid against tetrachloro-carbon (CCl_4) hepatotoxicity in male rats by the synthesis of silver nanoparticles (AgNPs). *Molecules*, *27*(23), 8308.

Al-Baqami, N. M., & Hamza, R. Z. (2021). Synergistic antioxidant capacities of vanillin and chitosan nanoparticles against reactive oxygen species, hepatotoxicity, and genotoxicity induced by aging in male Wistar rats. *Human & Experimental Toxicology*, *40*(1), 183-202.

Alhadid, A., Bustanji, Y., Harb, A., Al-Hiari, Y., & Abdalla, S. (2022). Vanillic acid inhibited the induced glycation using in vitro and in vivo models. *Evidence-Based Complementary and Alternative Medicine*, *2022*(1), 7119256.

Almostafa, M. M., Mohamed, M. E., & Younis, N. S. (2024). Ameliorative effects of vanillin against pentylenetetrazole-induced epilepsy and associated memory loss in mice: the role of Nrf2/HO-1/NQO1 and HMGB1/RAGE/TLR4/NFκB pathways. *International Immunopharmacology*, *129*, 111657.

Anand, A., Khurana, N., Ali, N., AlAsmari, A. F., Alharbi, M., Waseem, M., & Sharma, N. (2022). Ameliorative effect of vanillin on scopolamine-induced dementia-like cognitive impairment in a mouse model. *Frontiers in Neuroscience*, *16*, 1005972.

Anderson, M. C., & Floresco, S. B. (2022). Prefrontal-hippocampal interactions supporting the extinction of emotional memories: model. Neuropsychopharmacology, 47(1), 180-195.

Arya, S. S., Rookes, J. E., Cahill, D. M., & Lenka, S. K. (2021). Vanillin: a review on the therapeutic prospects of a popular flavouring molecule. *Advances in traditional medicine*, *21*(3), 1-17.

Baj, J., Flieger, W., Barbachowska, A., Kowalska, B., Flieger, M., Forma, A., Teresiński, G., Portincasa, P., Buszewicz, G., Radzikowska-Büchner, E., & Flieger, J. (2023). Consequences of disturbing manganese homeostasis. *International journal of molecular sciences*, *24*(19), 14959.

Balaram, V. (2022). Sources and applications of rare earth elements. *Environmental Technologies to Treat Rare Earth Elements Pollution: Principles and Engineering; IWA Publishing: London, UK*, *113*, 75-113.

Baumann, O., & Mattingley, J. B. (2021). Extrahippocampal contributions to spatial navigation in humans: A review of the neuroimaging evidence. Hippocampus, 31(7), 640-657.

Bergeron, S., Champoux-Ouellet, É., Samson, N., Doyon, M., Geoffroy, M., Farkouh, A., Bertelle, V., Massé, É., Cloutier, S., & Praud, J. P. (2024). Effects of vanilla odor on hypoxia-related periodic breathing in premature newborns: A pilot study. *Archives de Pédiatrie*, *31*(6), 369-373.

Bezerra-Filho, C. S., Barboza, J. N., Souza, M. T., Sabry, P., Ismail, N. S., & de Sousa, D. P. (2019). Therapeutic potential of vanillin and its main metabolites to regulate the inflammatory response and oxidative stress. *Mini reviews in medicinal chemistry*, *19*(20), 1681-1693.

Bhushan, R., Ravichandiran, V., & Kumar, N. (2022). An overview of the anatomy and physiology of the brain. Nanocarriers for Drug-Targeting Brain Tumors, 3-29.

Buege J.A., and Aust S.D. 1978. Microsomal lipid peroxidation. Method in Enzymology, 52, 302-310.

Buss, E. W., Corbett, N. J., Roberts, J. G., Ybarra, N., Musial, T. F., Simkin, D., Molina Campos, E., Oh, K.J., Nielsen, L.L., Ayala, G.D., Mullen, S.A., & Nicholson, D. A. (2021). Cognitive aging is associated with redistribution of synaptic weights in the hippocampus. Proceedings of the National Academy of Sciences, 118(8), e1921481118.

Cao, J., Wu, Q., Liu, X., Zhu, X., Huang, C., Wang, X., & Song, Y. (2025). Mechanistic insight on nanomaterial-induced reactive oxygen species formation. *Journal of Environmental Sciences*, *151*, 200-210.

Carobrez, A. P., & Bertoglio, L. J. (2005). Ethological and temporal analyses of anxiety-like behavior: the elevated plus-maze model 20 years on. *Neuroscience & Biobehavioral Reviews*, *29*(8), 1193-1205.

Carstens, M. H., & Sarnat, H. B. (2023). The Neuromeric System: Segmentation of the Neural Tube. In The Embryologic Basis of Craniofacial Structure: Developmental Anatomy, Evolutionary Design, and Clinical Applications (pp. 241-309). Cham: Springer International Publishing.

Catani, M. (2022). The connectional anatomy of the temporal lobe. Handbook of clinical neurology, 187, 3-16.

Chakravarthi, S. S., Monroy-Sosa, A., & Elisevich, K. (2025). The Diencephalon: Dorsal Thalamus. In From Anatomy to Function of the Central Nervous System (pp. 255-284). Academic Press.

Chandra, S., & Roychoudhury, A. (2020). Role of selenium and manganese in mitigating oxidative damages. *Protective chemical agents in the amelioration of plant abiotic stress: Biochemical and Molecular Perspectives*, 597-621.

Chauhan, P., Jethwa, K., Rathawa, A., Chauhan, G., & Mehra, S. (2021). The anatomy of the hippocampus. *Exon Publications*, 17-30.

Chen, B., Zhao, J., Zhang, R., Zhang, L., Zhang, Q., Yang, H., & An, J. (2022). Neuroprotective effects of natural compounds on neurotoxin-induced oxidative stress and cell apoptosis. *Nutritional neuroscience, 25*(5), 1078-1099.

Cheng, H., Villahoz, B. F., Ponzio, R. D., Aschner, M., & Chen, P. (2023). Signaling pathways involved in Manganese-Induced neurotoxicity. *Cells, 12*(24), 2842.

Chib, S., & Singh, S. (2022). Manganese and related neurotoxic pathways: A potential therapeutic target in neurodegenerative diseases. *Neurotoxicology and teratology*, *94*, 107124.

Choi, S., Haam, C. E., Oh, E. Y., Byeon, S., Choi, S. K., & Lee, Y. H. (2022). Vanillin induces relaxation in rat mesenteric resistance arteries by inhibiting extracellular Ca2+ influx. *Molecules*, *28*(1), 288.

Cohen, A. O., & Meyer, H. C. (2020). Ventral hippocampus projections to prelimbic cortex support contextual fear memory. *The Journal of Neuroscience*, *40*(44), 8410.

Cohen, G., Dembiec, D. and Marcus, J. (1970). Measurement of catalase activity in tissue extracts. Analytical biochemistry. 34: 30 - 38.

Cox, A., Brown, K. C., & Valentovic, M. A. (2024). The E-liquid flavoring vanillin alters energy and autophagic pathways in human proximal tubule (HK-2) epithelial cells. *Chemico-Biological Interactions, 394*, 111003.

Crossley, C. A., Omoluabi, T., Torraville, S. E., Duraid, S., Maziar, A., Hasan, Z., Rajani, V., Ando, K., Hell, J.W., & Yuan, Q. (2024). Hippocampal hyperphosphorylated tau induced deficiency is rescued by L-type calcium channel blockade. Brain communications, 6(2), fcae096.

Danieli, K., Guyon, A., & Bethus, I. (2023). Episodic Memory formation: A review of complex Hippocampus input pathways. Progress in Neuro-Psychopharmacology and Biological Psychiatry, 126, 110757.

De Brouwer, G., Fick, A., Harvey, B. H., & Wolmarans, D. W. (2019). A critical inquiry into marble-burying as a preclinical screening paradigm of relevance for anxiety and obsessive–compulsive disorder: Mapping the way forward. *Cognitive, Affective, & Behavioral Neuroscience*, *19*(1), 1-39.

de Figueiredo Cerqueira, M. M., Castro, M. M. L., Vieira, A. A., Kurosawa, J. A. A., do Amaral Junior, F. L., de Siqueira, F. D. C. C., & Sosthenes, M. C. K. (2023). Comparative analysis between Open Field and Elevated Plus Maze tests as a method for evaluating anxiety-like behavior in mice. *Heliyon*, *9*(4).

de Oliveira, R. T., da Silva Oliveira, J. P., & Macedo, A. F. (2022). Vanilla beyond Vanilla planifolia and Vanilla× tahitensis: Taxonomy and historical notes, reproductive biology, and metabolites. *Plants*, *11*(23), 3311.

De, A. K., & De, M. (2022). Functional and therapeutic applications of some general and rare spices. In *Functional foods and nutraceuticals in metabolic and non-communicable diseases* (pp. 411-420). Academic Press.

Demirbağ, B., Yildirim, M., Cimentepe, M., Necip, A., Unver, H., & Tiftik, E. N. (2025). Novel vanillin-derived Schiff Bases: Synthesis, characterization, antibacterial activity, enzyme inhibition, antioxidant activity, anti-inflammatory activity on LPS-induced RAW264. 7 macrophage cell line, and In Silico studies. *Journal of Molecular Structure*, *1338*, 142320.

Dey, S., Tripathy, B., Kumar, M. S., & Das, A. P. (2023). Ecotoxicological consequences of manganese mining pollutants and their biological remediation. *Environmental chemistry and ecotoxicology*, *5*, 55-61.

Donato, F., Alberini, C. M., Amso, D., Dragoi, G., Dranovsky, A., & Newcombe, N. S. (2021). The ontogeny of hippocampus-dependent memories. Journal of Neuroscience, 41(5), 920-926.

Dos Santos, A. M., Andrade, V., & Aschner, M. (2017). Neuroprotective and Therapeutic Strategies for Manganese–Induced Neurotoxicity. *Clinical pharmacology and translational medicine*, *1*(2), 54.

Drury, R. A. B., and Wallington, E. A. (1980). General Staining Procedures. *In: R.A.B. Drury and E.A. Wallington (Eds.),* Carleton's Histological Techniques, 125-150. Oxford University Press, Oxford.

Du, L., Xiao, L., Zou, C., & Huang, J. (2022). Vanillin attenuates the ethanol withdrawal syndrome and ethanol withdrawal induced anxiety by regulating the neurochemical balance. *Folia Neuropathologica*, *60*(3), 316-323.

Elseweidy, M. M., Ali, S. I., Shaheen, M. A., Abdelghafour, A. M., & Hammad, S. K. (2023). Vanillin and pentoxifylline ameliorate isoproterenol-induced myocardial injury in rats via the Akt/HIF-1α/VEGF signaling pathway. *Food & Function*, *14*(7), 3067-3082.

Engwa, G. A., Nweke, F. N., & Nkeh-Chungag, B. N. (2022). Free radicals, oxidative stress-related diseases and antioxidant supplementation. *Alternative Therapies in Health & Medicine*, *28*(1).

Enogieru, A., & Omoruyi, S. (2022). Exploration of aqueous Phyllanthus amarus leaf extract as a protective agent in mercury chloride-exposed wistar rats: A neurobehavioural study. *Journal of Applied Sciences and Environmental Management*, *26*(4), 629-637.

Estela-Pro, V. J., & Burwell, R. D. (2022). The anatomy and function of the postrhinal cortex. Behavioral neuroscience, 136(2), 101.

Etter, G., Carmichael, J. E., & Williams, S. (2023). Linking temporal coordination of hippocampal activity to memory function. Frontiers in Cellular Neuroscience, 17, 1233849.

Eva, L., Brehar, F. M., Florian, I. A., Covache-Busuioc, R. A., Costin, H. P., Dumitrascu, D. I., Bratu, B.G., Glavan, L.A., & Ciurea, A. V. (2023). Neuropsychiatric and neuropsychological aspects of alcohol-related cognitive disorders: An in-depth review of Wernicke's encephalopathy and Korsakoff's syndrome. Journal of clinical medicine, 12(18), 6101.

Farag, S. M., Omar, N. A., & El-Gammal, H. L. (2024). Ameliorative Effects of Vitamin C and Vanillin against Potassium Bromate Toxicity in Male Albino Rats: Biochemical, Hematological and Histological Study. *Egyptian Journal of Histology*, *47*(2), 725-738.

Farzan, M., Farzan, M., Amini-Khoei, H., Shahrani, M., Bijad, E., Anjomshoa, M., & Shabani, S. (2023). Protective effects of vanillic acid on autistic-like behaviors in a rat model of maternal separation stress: Behavioral, electrophysiological, molecular and histopathological alterations. *International immunopharmacology*, *118*, 110112.

Fayeulle, A., Trudel, E., Damiens, A., Josse, A., Youssef, N. B. H., Vigneron, P., Vayssade, M., Rossi, C., & Ceballos, C. (2021). Antimicrobial and antioxidant activities of amines derived from vanillin as potential preservatives: Impact of the substituent chain length and polarity. *Sustainable Chemistry and Pharmacy*, *22*, 100471.

Fernandes, J., Uppal, K., Liu, K. H., Hu, X., Orr, M., Tran, V., Go, Y.M., & Jones, D. P. (2023). Antagonistic interactions in mitochondria ROS signaling responses to manganese. *Antioxidants*, *12*(4), 804.

Fernández-Olmo, I., Mantecón, P., Markiv, B., Ruiz-Azcona, L., & Santibáñez, M. (2020). A review on the environmental exposure to airborne manganese, biomonitoring, and neurological/neuropsychological outcomes. *Reviews of Environmental Contamination and Toxicology Volume 254*, 85-130.

Flora, S. J. S., Shrivastava, R., & Mittal, M. (2013). Chemistry and pharmacological properties of some natural and synthetic antioxidants for heavy metal toxicity. *Current medicinal chemistry*, *20*(36), 4540-4574.

Fouad, A. A., & Al-Melhim, W. N. (2018). Vanillin mitigates the adverse impact of cisplatin and methotrexate on rat kidneys. *Human & experimental toxicology*, *37*(9), 937-943.

Fujimaki, S., Sakamoto, S., Shimada, S., Kino, K., & Furuya, T. (2024). Engineering a coenzyme-independent dioxygenase for one-step production of vanillin from ferulic acid. *Applied and Environmental Microbiology*, *90*(6), e00233-24.

Gaikwad, V., Rautela, A., Kedare, G., Sarkar, S., Pal, R. P., & Sharma, A. (2024). Role of Flavoured Additives in Ruminant Production. In *Feed Additives and Supplements for Ruminants* (pp. 265-279). Singapore: Springer Nature Singapore.

Gallage, N. J., & Møller, B. L. (2017). Vanilla: The most popular flavour. In *Biotechnology of natural products* (pp. 3-24). Cham: Springer International Publishing.

Gandhi, D., Rudrashetti, A. P., & Rajasekaran, S. (2022). The impact of environmental and occupational exposures of manganese on pulmonary, hepatic, and renal functions. *Journal of Applied Toxicology*, *42*(1), 103-129.

Genon, S., Bernhardt, B. C., La Joie, R., Amunts, K., & Eickhoff, S. B. (2021). The many dimensions of human hippocampal organization and (dys) function. Trends in neurosciences, 44(12), 977-989.

Gliebus, G. P. (2018). Memory dysfunction. *Continuum*, *24*(3), 727-744.

Gomes, C. S., & Silva, E. A. (2021). Health benefits and risks of minerals: bioavailability, bio-essentiality, toxicity, and pathologies. In *Minerals Latu Sensu and Human Health: Benefits, Toxicity and Pathologies* (pp. 81-179). Cham: Springer International Publishing.

González-Arnay, E., Pérez-Santos, I., Jiménez-Sánchez, L., Cid, E., Gal, B., de la Prida, L. M., & Cavada, C. (2024). Immunohistochemical field parcellation of the human hippocampus along its antero-posterior axis. Brain Structure and Function, 229(2), 359-385.

Gu, Y., Yu, J., Ding, C., Zhou, Y., Yang, J., Yu, W., Zhang, X., & Huang, H. (2021). Flavonoid GL-V9 suppresses invasion and migration of human colorectal cancer cells by inhibiting PI3K/Akt and MMP-2/9 signaling. *Journal of Cancer*, *12*(15), 4542.

Guan, R., Wang, T., Dong, X., Du, K., Li, J., Zhao, F., & Chen, R. (2022). Effects of co-exposure to lead and manganese on learning and memory deficits. *Journal of Environmental Sciences*, *121*, 65-76.

Gul, Q., Karim, N., Shoaib, M., Zahoor, M., Rahman, M. U., Bilal, H., Ullah, R., & Alotaibi, A. (2024). Vanillin derivatives as antiamnesic agents in scopolamine-induced memory impairment in mice. *Heliyon*, *10*(4).

Gurol, K. C., Aschner, M., Smith, D. R., & Mukhopadhyay, S. (2022). Role of excretion in manganese homeostasis and neurotoxicity: A historical perspective. *American Journal of Physiology-Gastrointestinal and Liver Physiology*, *322*(1), G79-G92.

Harischandra, D. S., Ghaisas, S., Zenitsky, G., Jin, H., Kanthasamy, A., Anantharam, V., & Kanthasamy, A. G. (2019). Manganese-induced neurotoxicity: new insights into the triad of protein misfolding, mitochondrial impairment, and neuroinflammation. *Frontiers in neuroscience*, *13*, 654.

Hayes, G., Laurel, M., MacKinnon, D., Zhao, T., Houck, H. A., & Becer, C. R. (2022). Polymers without petrochemicals: sustainable routes to conventional monomers. *Chemical Reviews*, *123*(5), 2609-2734.

Iannuzzi, C., Liccardo, M., & Sirangelo, I. (2023). Overview of the role of vanillin in neurodegenerative diseases and neuropathophysiological conditions. *International Journal of Molecular Sciences*, *24*(3), 1817.

Ijomone, O. M., Ifenatuoha, C. W., Aluko, O. M., Ijomone, O. K., & Aschner, M. (2020). The aging brain: impact of heavy metal neurotoxicity. *Critical reviews in toxicology*, *50*(9), 801-814.

Inoue, Y., Shue, F., Bu, G., & Kanekiyo, T. (2023). Pathophysiology and probable etiology of cerebral small vessel disease in vascular dementia and Alzheimer’s disease. Molecular neurodegeneration, 18(1), 46.

Jomova, K., Alomar, S. Y., Nepovimova, E., Kuca, K., & Valko, M. (2025). Heavy metals: toxicity and human health effects. *Archives of toxicology*, *99*(1), 153-209.

Kafali, M., Finos, M. A., & Tsoupras, A. (2024). Vanillin and its derivatives: a critical review of their anti-inflammatory, anti-infective, wound-healing, neuroprotective, and anti-cancer health-promoting benefits. *Nutraceuticals*, *4*(4), 522-561.

Kalisch, R., Russo, S. J., & Müller, M. B. (2024). Neurobiology and systems biology of stress resilience. Physiological reviews, 104(3), 1205-1263.

Kamali, A., Milosavljevic, S., Gandhi, A., Lano, K. R., Shobeiri, P., Sherbaf, F. G., Sair, H.I., Riascos, R.F., & Hasan, K. M. (2023). The cortico-limbo-thalamo-cortical circuits: An update to the original papez circuit of the human limbic system. Brain topography, 36(3), 371-389.

Kamaly, N. A., Kamel, A. S., Sadik, N. A., & Shahin, N. N. (2025). Milnacipran and vanillin alleviate fibromyalgia-associated depression in reserpine-induced rat model: role of Wnt/β-catenin signaling. *Molecular Neurobiology*, *62*(6), 7682-7705.

Kapoor, B., Gulati, M., Gupta, R., Singh, S. K., Gupta, M., Nabi, A., & Chawla, P. A. (2021). A review on plant flavonoids as potential anticancer agents. *Current Organic Chemistry*, *25*(6), 737-747.

Kim, H., Harrison, F. E., Aschner, M., & Bowman, A. B. (2022). Exposing the role of metals in neurological disorders: a focus on manganese. *Trends in molecular medicine*, *28*(7), 555-568.

Kim, M. E., Na, J. Y., Park, Y. D., & Lee, J. S. (2019). Anti-neuroinflammatory effects of vanillin through the regulation of inflammatory factors and NF-κB signaling in LPS-stimulated microglia. *Applied Biochemistry and Biotechnology*, *187*(3), 884-893.

Kolling, W. M., & Ghosh, T. K. (2021). Oral liquid dosage forms: Solutions, elixirs, syrups, suspensions, and emulsions. In *Theory and Practice of Contemporary Pharmaceutics* (pp. 367-385). CRC Press.

Kominami, R., Sonomura, T., Ito, T., Shinohara, H., Kishibe, M., Uemura, M., & Honma, S. (2023). Three-dimensional anatomical structure formed by granule cell layer and pyramidal cell layer in human hippocampus. Anatomical Science International, 98(1), 66-76.

Kulshreshtha, D., Ganguly, J., & Jog, M. (2021). Manganese and movement disorders: a review. *Journal of movement disorders*, *14*(2), 93.

Kumar, G. S., Sholapuri, P., K, D., Shaily Enugonda, M., & BP, G. (2025). In vivo and in silico anti-inflammatory activity of Artemisia vulgaris and β-caryophyllene oxide in carrageenan-induced paw edema in Wistar rats. *Drug and Chemical Toxicology*, *48*(2), 426-439.

Kundu, A. (2017). Vanillin biosynthetic pathways in plants. *Planta*, *245*(6), 1069-1078.

Lang, M., Colby, S., Ashby-Padial, C., Bapna, M., Jaimes, C., Rincon, S. P., & Buch, K. (2024). An imaging review of the hippocampus and its common pathologies. Journal of Neuroimaging, 34(1), 5-25.

Lechin, F., van der Dijs, B., Amat, J., & Lechin, M. (2020). Neuroanatomical basis. In *Neurochemistry & Clinical Disorders* (pp. 1-48). CRC Press.

Li, L., & Yang, X. (2018). The essential element manganese, oxidative stress, and metabolic diseases: links and interactions. *Oxidative medicine and cellular longevity*, *2018*(1), 7580707.

Li, Q., & Zhu, X. (2021). Vanillin and its derivatives, potential promising antifungal agents, inhibit Aspergillus flavus spores via destroying the integrity of cell membrane rather than cell wall. *Grain & oil science and technology*, *4*(2), 54-61.

Liu, F., Wang, Z., Wei, Y., Liu, R., Jiang, C., Gong, C., Liu, Y., & Yan, B. (2021). The leading role of adsorbed lead in PM2. 5-induced hippocampal neuronal apoptosis and synaptic damage. Journal of hazardous materials, 416, 125867.

Lucifero, A. G., Baldoncini, M., Bruno, N., Tartaglia, N., Ambrosi, A., Marseglia, G. L., Galzio, R., Campero, A., Hernesniemi, J., & Luzzi, S. (2021). Microsurgical neurovascular anatomy of the brain: the anterior circulation (part I). Acta Bio Medica: Atenei Parmensis, 92(Suppl 4), e2021412.

Lueptow, L. M. (2017). Novel object recognition test for the investigation of learning and memory in mice. *Journal of visualized experiments: JoVE*, (126), 55718.

Lupien, S. J., Juster, R. P., Raymond, C., & Marin, M. F. (2018). The effects of chronic stress on the human brain: From neurotoxicity, to vulnerability, to opportunity. *Frontiers in neuroendocrinology*, *49*, 91-105.

Ma, Q., Liu, L., Zhao, S., Huang, Z., Li, C., Jiang, S., Li, Q., & Gu, P. (2022). Biosynthesis of vanillin by different microorganisms: a review. *World Journal of Microbiology and Biotechnology*, *38*(3), 40.

Ma, Z., Liu, K., Li, X. R., Wang, C., Liu, C., Yan, D. Y., & Xu, B. (2020). Alpha-synuclein is involved in manganese-induced spatial memory and synaptic plasticity impairments via TrkB/Akt/Fyn-mediated phosphorylation of NMDA receptors. *Cell death & disease*, *11*(10), 834.

Malik, D., Narayanasamy, N., Pratyusha, V. A., Thakur, J., & Sinha, N. (2023). Microminerals and toxic heavy metals. In *Textbook of nutritional biochemistry* (pp. 447-504). Singapore: Springer Nature Singapore.

Manavalan, R. K., Enoch, K., Volegov, A. S., Angusamy, G., & Nallasivam, S. (2024). Review on medical applications of manganese oxide (Mn2+, Mn3+, and Mn4+) magnetic nanoparticles. *Journal of Nanomaterials*, *2024*(1), 1073915.

McGough, D., & Jardine, L. (2017). A two-generation inhalation reproductive toxicity study upon the exposure to manganese chloride. *Neurotoxicology*, *58*, 194-202.

Mezzaroba, L., Alfieri, D. F., Simão, A. N. C., & Reiche, E. M. V. (2019). The role of zinc, copper, manganese and iron in neurodegenerative diseases. *Neurotoxicology*, *74*, 230-241.

Mezzaroba, L., Alfieri, D. F., Simão, A. N. C., & Reiche, E. M. V. (2019). The role of zinc, copper, manganese and iron in neurodegenerative diseases. *Neurotoxicology*, *74*, 230-241.

Misra, H.P. and Fridovich, I. (1972). The role of superoxide anion in the autoxidation of epinephrine and a simple assay for superoxide dismutase. *The Journal of Biological Chemistry*. 247(10), 3170 - 3175.

Mithani, K., Davison, B., Meng, Y., & Lipsman, N. (2020). The anterior limb of the internal capsule: Anatomy, function, and dysfunction. *Behavioural brain research*, *387*, 112588.

More, A., Elder, T., & Jiang, Z. (2021). A review of lignin hydrogen peroxide oxidation chemistry with emphasis on aromatic aldehydes and acids. *Holzforschung*, *75*(9), 806-823.

Naoi, M., Wu, Y., Shamoto-Nagai, M., & Maruyama, W. (2019). Mitochondria in neuroprotection by phytochemicals: Bioactive polyphenols modulate mitochondrial apoptosis system, function and structure. *International journal of molecular sciences*, *20*(10), 2451.

Nyarko-Danquah, I., Pajarillo, E., Digman, A., Soliman, K. F., Aschner, M., & Lee, E. (2020). Manganese accumulation in the brain via various transporters and its neurotoxicity mechanisms. *Molecules*, *25*(24), 5880.

Nyman, N. (1959). Determination of glutathione peroxidase in tissue. *Analytical Biochemistry*, 28, 481.

Obeng, S. K., Kulhánek, M., Balík, J., Černý, J., & Sedlář, O. (2024). Manganese: from soil to human health—a comprehensive overview of its biological and environmental significance. *Nutrients*, *16*(20), 3455.

Ogunro, O. B., & Olasehinde, O. R. (2024). Neuroinflammatory response and redox-regulation activity of Hyperoside in manganese-induced neurotoxicity model of Wistar rats. *Current Aging Science*, *17*(3), 220-236.

Ohara, S., Rannap, M., Tsutsui, K. I., Draguhn, A., Egorov, A. V., & Witter, M. P. (2023). Hippocampal-medial entorhinal circuit is differently organized along the dorsoventral axis in rodents. Cell reports, 42(1).

Ohiagu, F. O., Chikezie, P. C., Ahaneku, C. C., & Chikezie, C. M. (2022). Human exposure to heavy metals: toxicity mechanisms and health implications. *Material Science & Engineering International Journal*, *6*(2), 78-87.

Okar, S. V., Fagiani, F., Absinta, M., & Reich, D. S. (2024). Imaging of brain barrier inflammation and brain fluid drainage in human neurological diseases. Cellular and Molecular Life Sciences, 81(1), 31.

Ota, T. (2024). Functional cerebral venous anatomy from the viewpoint of venous collaterals Part I, supratentorial superficial and deep venous system. Stroke: Vascular and Interventional Neurology, 4(2), e001050.

Pajarillo, E., Nyarko-Danquah, I., Digman, A., Multani, H. K., Kim, S., Gaspard, P., Aschner, M., & Lee, E. (2022). Mechanisms of manganese-induced neurotoxicity and the pursuit of neurotherapeutic strategies. *Frontiers in pharmacology*, *13*, 1011947.

Peres, T. V., Schettinger, M. R. C., Chen, P., Carvalho, F., Avila, D. S., Bowman, A. B., & Aschner, M. (2016). Manganese-induced neurotoxicity: a review of its behavioral consequences and neuroprotective strategies. *BMC Pharmacology and Toxicology*, *17*(1), 57.

Petrovic, S., Arsic, A., Ristic-Medic, D., Cvetkovic, Z., & Vucic, V. (2020). Lipid peroxidation and antioxidant supplementation in neurodegenerative diseases: a review of human studies. *Antioxidants*, *9*(11), 1128.

Pourhadi, M., Ghasemi, A., Abediny, R., Javanmard, S. H., & Vaseghi, G. (2022). The inhibitory effects of vanillin on the growth of melanoma by reducing nuclear factor-κB activation. *Advanced Biomedical Research*, *11*(1), 68.

Raj, N. D., & Singh, D. (2022). A critical appraisal on ferulic acid: Biological profile, biopharmaceutical challenges and nano formulations. *Health Sciences Review*, *5*, 100063.

Rajak, C., Singh, N., & Parashar, P. (2020). Metal toxicity and natural antidotes: prevention is better than cure. *Environmental Science and Pollution Research*, *27*(35), 43582-43598.

Raju, S. K., Sundhararajan, N., Sekar, P., & Nagalingam, Y. (2023). Therapeutic aspects of biologically potent vanillin derivatives: A critical. *Journal of Drug Delivery & Therapeutics*, *13*(7), 177-189.

Rakoczy, K., Szlasa, W., Saczko, J., & Kulbacka, J. (2021). Therapeutic role of vanillin receptors in cancer. *Advances in Clinical and Experimental Medicine*, *30*(12), 1293-1301.

Rani, L., & Mondal, A. C. (2024). Vanillin Mitigates the MPTP-Induced α-Synucleinopathy in a Mouse Model of Parkinson's Disease: Insights into the Involvement of Wnt/β-Catenin Signaling. *Journal of Integrative Neuroscience*, *23*(9), 175.

Rao, Y. L., Ganaraja, B., Murlimanju, B. V., Joy, T., Krishnamurthy, A., & Agrawal, A. (2022). Hippocampus and its involvement in Alzheimer’s disease: a review. 3 Biotech, 12(2), 55.

Razaq, N., Asghar, A., Mumtaz, A., Al-Mijalli, S. H., Nisa, M. U., Riaz, T., Iqbal, M., & Shahid, B. (2024). Synthesis of biologically active cefpodoxime and vanillin-based schiff base metal complexes with the detailed biological evaluations. *BioMetals*, *37*(5), 1201-1224.

Richards, I. N., & Richards, J. R. (2020). Does manganese contribute to methamphetamine-induced psychosis?. *Current Emergency and Hospital Medicine Reports*, *8*(4), 133-141.

Rojas-García, A., Fernández-Ochoa, Á., Cádiz-Gurrea, M. D. L. L., Arráez-Román, D., & Segura-Carretero, A. (2023). Neuroprotective effects of agri-food by-products rich in phenolic compounds. *Nutrients*, *15*(2), 449.

Rolls, E. T., & Treves, A. (2024). A theory of hippocampal function: new developments. Progress in Neurobiology, 102636.

Rolls, E. T., Deco, G., Huang, C. C., & Feng, J. (2022). The effective connectivity of the human hippocampal memory system. Cerebral Cortex, 32(17), 3706-3725.

Roy, T., Pal, N., & Das, N. (2024). Biochemical, Biosynthetic and Biotechnological Approaches for an Orchid-Derived Natural Flavoring and Therapeutic Agent Vanillin-A Review. *The Chemistry inside Spices & Herbs: Research and Development: Volume 3*, 66-108.

Sachdev, S., Ansari, S. A., Ansari, M. I., Fujita, M., & Hasanuzzaman, M. (2021). Abiotic stress and reactive oxygen species: Generation, signaling, and defense mechanisms. *Antioxidants*, *10*(2), 277.

Sakhaie, N., Sadegzadeh, F., Mohammadnia, A., Dadkhah, M., & Saadati, H. (2020). Sex-dependent effects of postweaning exposure to an enriched environment on novel objective recognition memory and anxiety-like behaviors: The role of hippocampal BDNF level. *International Journal of Developmental Neuroscience*, *80*(5), 396-408.

Salam, M. A., Al-Amin, M. Y., Salam, M. T., Pawar, J. S., Akhter, N., Rabaan, A. A., & Alqumber, M. A. (2023, July). Antimicrobial resistance: a growing serious threat for global public health. In *Healthcare* (Vol. 11, No. 13, p. 1946). MDPI.

Salau, V. F., & Islam, M. S. (2024). Vanillin: a natural phenolic compound with neuroprotective benefits. In *Natural Molecules in Neuroprotection and Neurotoxicity* (pp. 1857-1879). Academic Press.

Salau, V. F., Erukainure, O. L., Ibeji, C. U., Olasehinde, T. A., Koorbanally, N. A., & Islam, M. S. (2020). Vanillin and vanillic acid modulate antioxidant defense system via amelioration of metabolic complications linked to Fe2+-induced brain tissues damage. *Metabolic Brain Disease*, *35*(5), 727-738.

Salimi, A., Haddadi, S., Khezri, S., Asgari, B., & Pourgholi, M. (2024). Vanillic acid protects mortality and toxicity induced by N-ethyl-N-nitrosourea in mice; in vivo model of chronic lymphocytic leukemia. *Toxicology Reports*, *12*, 389-396.

Salta, E., Lazarov, O., Fitzsimons, C. P., Tanzi, R., Lucassen, P. J., & Choi, S. H. (2023). Adult hippocampal neurogenesis in Alzheimer's disease: A roadmap to clinical relevance. Cell Stem Cell, 30(2), 120-136.

Santos, L. D., Lautru, S., & Pernodet, J. L. (2024). Genetic Engineering Approaches for the Microbial Production of Vanillin. *Biomolecules*, *14*(11), 1413.

Sefi, M., Elwej, A., Chaâbane, M., Bejaoui, S., Marrekchi, R., Jamoussi, K., Gouiaa, N., Boudawara-Sellemi, T., El Cafsi, M., Zeghal, N., & Soudani, N. (2019). Beneficial role of vanillin, a polyphenolic flavoring agent, on maneb-induced oxidative stress, DNA damage, and liver histological changes in Swiss albino mice. *Human & experimental toxicology*, *38*(6), 619-631.

Semyachkina-Glushkovskaya, O. V., Postnov, D. E., Khorovodov, A. P., Navolokin, N. A., & Kurthz, J. H. G. (2023). Lymphatic drainage system of the brain: a New player in neuroscience. Journal of Evolutionary Biochemistry and Physiology, 59(1), 1-19.

Shah, H. E., Bhawnani, N., Ethirajulu, A., Alkasabera, A., Onyali, C. B., Anim-Koranteng, C., & Mostafa, J. A. (2021). Iron deficiency-induced changes in the hippocampus, corpus striatum, and monoamines levels that lead to anxiety, depression, sleep disorders, and psychotic disorders. Cureus, 13(9).

Sheintuch, L., Geva, N., Deitch, D., Rubin, A., & Ziv, Y. (2023). Organization of hippocampal CA3 into correlated cell assemblies supports a stable spatial code. Cell reports, 42(2).

Singh, N., Savanur, M. A., Srivastava, S., D'Silva, P., & Mugesh, G. (2019). A manganese oxide nanozyme prevents the oxidative damage of biomolecules without affecting the endogenous antioxidant system. *Nanoscale*, *11*(9), 3855-3863.

Slotnick, S. D. (2022). The hippocampus and long-term memory. Cognitive Neuroscience, 13(3-4), 113-114.

Strasser, A., Xin, L., Gruetter, R., & Sandi, C. (2019). Nucleus accumbens neurochemistry in human anxiety: A 7 T 1H-MRS study. *European neuropsychopharmacology*, *29*(3), 365-375.

Sviridova, V. M., Ivlev, A. P., Kaik, E. A., Karpenko, M. N., & Ivleva, I. S. (2025). Manganese-induced damage to the serotoninergic system is associated with the development of anxiety and depression. *Toxicology Reports*, *14*, 102001.

Tarnacka, B., Jopowicz, A., & Maślińska, M. (2021). Copper, iron, and manganese toxicity in neuropsychiatric conditions. *International journal of molecular sciences*, *22*(15), 7820.

Tartt, A. N., Mariani, M. B., Hen, R., Mann, J. J., & Boldrini, M. (2022). Dysregulation of adult hippocampal neuroplasticity in major depression: pathogenesis and therapeutic implications. Molecular psychiatry, 27(6), 2689-2699.

Tazon, A. W., Awwad, F., Meddeb-Mouelhi, F., & Desgagné-Penix, I. (2024). Biotechnological advances in vanillin production: from natural vanilla to metabolic engineering platforms. *BioChem*, *4*(4), 323-349.

Thorne, R. G., de Lange, E. C. M., Hammarlund-Udenaes, M., & Thorne, R. G. (2022). Central Nervous System Anatomy and Physiology: Structure-Function Relationships, Blood Supply, Ventricles, and Brain Fluids. Drug Delivery to the Brain Physiological Concepts, Methodologies and Approaches, 33, 763-790.

Timme-Laragy, A. R., Di Giulio, R. T., & Meyer, J. N. (2024). Reactive oxygen species and redox stress. In *Toxicology of Fishes* (pp. 121-155). CRC Press.

Turner, V. S., O'Sullivan, R. O., & Kheirbek, M. A. (2022). Linking external stimuli with internal drives: A role for the ventral hippocampus. Current opinion in neurobiology, 76, 102590.

Uddin, L. Q. (2021). Cognitive and behavioural flexibility: neural mechanisms and clinical considerations. Nature Reviews Neuroscience, 22(3), 167-179.

Ueno, H., Shimada, A., Suemitsu, S., Murakami, S., Kitamura, N., Wani, K., Takahashi, Y., Matsumoto, Y., Okamoto, M., Fujiwara, Y., & Ishihara, T. (2019). Comprehensive behavioral study of the effects of vanillin inhalation in mice. *Biomedicine & Pharmacotherapy*, *115*, 108879.

Valgimigli, L. (2023). Lipid peroxidation and antioxidant protection. *Biomolecules*, *13*(9), 1291.

Vandrey, B., Armstrong, J., Brown, C. M., Garden, D. L., & Nolan, M. F. (2022). Fan cells in lateral entorhinal cortex directly influence medial entorhinal cortex through synaptic connections in layer 1. Elife, 11, e83008.

Venkataraman, S., Athilakshmi, J. K., Rajendran, D. S., Bharathi, P., & Kumar, V. V. (2024). A comprehensive review of eclectic approaches to the biological synthesis of vanillin and their application towards the food sector. *Food Science and Biotechnology*, *33*(5), 1019-1036.

Wang, H., Yang, F., Xin, R., Cui, D., He, J., Zhang, S., & Sun, Y. (2020). The gut microbiota attenuate neuroinflammation in manganese exposure by inhibiting cerebral NLRP3 inflammasome. *Biomedicine & Pharmacotherapy*, *129*, 110449.

Wang, J., An, W., Wang, Z., Zhao, Y., Han, B., Tao, H., Wang, J., & Wang, X. (2024). Vanillin has potent antibacterial, antioxidant, and anti-inflammatory activities in vitro and in mouse colitis induced by multidrug-resistant Escherichia coli. *Antioxidants*, *13*(12), 1544.

Wegrzyn, D., Juckel, G., & Faissner, A. (2022). Structural and functional deviations of the hippocampus in schizophrenia and schizophrenia animal models. International Journal of Molecular Sciences, 23(10), 5482.

Wouk, J., Rechenchoski, D. Z., Rodrigues, B. C. D., Ribelato, E. V., & Faccin-Galhardi, L. C. (2021). Viral infections and their relationship to neurological disorders. Archives of Virology, 166, 733-753.

Xiao, K., Luo, Y., Liang, X., Tang, J., Wang, J., Xiao, Q., Qi, Y., Li, Y., Zhu, P., Yang, H., Xie, Y., & Tang, Y. (2021). Beneficial effects of running exercise on hippocampal microglia and neuroinflammation in chronic unpredictable stress-induced depression model rats. Translational psychiatry, 11(1), 461.

Xu, Y., Mohyeldin, A., Nunez, M. A., Doniz-Gonzalez, A., Vigo, V., Cohen-Gadol, A. A., & Fernandez-Miranda, J. C. (2021). Microvascular anatomy of the medial temporal region. Journal of Neurosurgery, 137(3), 747-759.

Yadav, P., Bhaduri, A., & Thakur, A. (2023). Manganese oxide nanoparticles: an insight into structure, synthesis and applications. *ChemBioEng Reviews*, *10*(4), 510-528.

Yalameha, B., Nejabati, H. R., & Nouri, M. (2023). Cardioprotective potential of vanillic acid. *Clinical and Experimental Pharmacology and Physiology*, *50*(3), 193-204.

Yan, D., Yang, Y., Lang, J., Wang, X., Huang, Y., Meng, J., Wu, J., Zeng, X., Li, H., Ma, H., & Gao, L. (2023). SIRT1/FOXO3-mediated autophagy signaling involved in manganese-induced neuroinflammation in microglia. *Ecotoxicology and environmental safety*, *256*, 114872.

Younis, N. N., Elsherbiny, N. M., Shaheen, M. A., & Elseweidy, M. M. (2020). Modulation of NADPH oxidase and Nrf2/HO-1 pathway by vanillin in cisplatin-induced nephrotoxicity in rats. *Journal of Pharmacy and Pharmacology*, *72*(11), 1546-1555.

Zhang, H., Jiang, X., Ma, L., Wei, W., Li, Z., Chang, S., Wen, J., Sun, J., & Li, H. (2022). Role of Aβ in Alzheimer's-related synaptic dysfunction. Frontiers in Cell and Developmental Biology, 10, 964075.

Zhao, L., & Palomero-Gallagher, N. (2025). Hippocampal architecture viewed through the eyes of methodological development. *Anatomical Science International*, 1-24.